A PRELIMINARY DESIGN TO INCLUDE A STABILITY AND CONTROL STUDY IN HOVERING FLIGHT OF A LATERALLY DISPOSED, SINGLE-BLADED, COUNTER-ROTATING, TWO-ROTOR HELICOPTER WITH SHROUDED TAIL PROPELLER

A THESIS

Presented to

the Faculty of the Graduate Division

by

William R. Ellis

In Partial Fulfillment

of the Requirements for the Degree

Master of Science in Aerospace Engineering

Georgia Institute of Technology

September, 1962

"In presenting the dissertation as a partial fulfillment of the requirements for an advanced degree from the Georgia Institute of Technology, I agree that the Library of the Institution shall make it available for inspection and circulation in accordance with its regulations governing materials of this type. I agree that permission to copy from, or to publish from, this dissertation may be granted by the professor under whose direction it was written, or, in his absence, by the dean of the Graduate Division when such copying or publication is solely for scholarly purposes and does not involve potential financial gain. It is understood that any copying from, or publication of, this dissertation which involves potential financial gain will not be allowed without written permission.

_____

72
12-R

A PRELIMINARY DESIGN TO INCLUDE A STABILITY AND CONTROL STUDY IN HOVERING FLIGHT OF A LATERALLY DISPOSED, SINGLE-BLADED, COUNTER-ROTATING, TWO-ROTOR HELICOPTER WITH SHROUDED TAIL PROPELLER

Approved:

Date Approved by Chairman: October 15, 1962

ACKNOWLEDGMENTS

The author wishes to express his most sincere appreciation to Professor Walter Castles, Jr. for suggesting the subject of this thesis and for his invaluable guidance. Gratitude is also extended to Doctor Robin B. Gray for his assistance in the preparation of this study and to Professor John J. Harper and Doctor Thomas W. Jackson for their review and comments on the material contained herein.

TABLE OF CONTENTS

LIST OF TABLES

LIST OF FIGURES

LIST OF SYMBOLS

a	Mean value of the lift curve slope
a'	Angle of lag between the resultant rotor thrust and the rotor tip-path plane
a_o	Rotor coning angle
a_1	Lateral component of the rotor blade pitch angle with respect to the tip-path plane
a_{1_s}	Lateral component of the rotor blade pitch angle with respect to the rotor mast axis
A	Aspect ratio of the wing
A_o	Mean blade collective pitch angle
b	Number of blades
c	Blade chord
c_{d_o}	Section profile drag coefficient
c_l	Section lift coefficient
C_D	Drag coefficient
C_{D_t}	Interference drag coefficient
C_f	Skin friction drag coefficient
$\overline{C}_L$	Mean lift coefficient
C_Q	Torque coefficient
$\Delta C_{Q_{a_o}}$	Increment to C_Q from terms involving blade coning
$\Delta C_{Q_{DP_c}}$	Increment to C_Q from constant profile drag
$\Delta C_{Q_{DP_v}}$	Increment to C_Q from variable profile drag
ΔC_{Q_L}	Increment to C_Q from lift
ΔC_{Q_s}	Increment to C_Q from tip stall on retreating blade

ΔC_{Q_t}	Increment to C_Q from blade tip losses
C_T	Thrust coefficient
C_X	Rotor X-force coefficient
$\Delta C_{X_{DP_c}}$	Increment to C_X from constant profile drag
$\Delta C_{X_{DP_v}}$	Increment to C_X from variable profile drag
ΔC_{X_L}	Increment to C_X from lift
C.W.	Rotor blade counter-weight
D	Drag
D_f	Composite drag
D_v	Vertical drag
f	Drag area
F_X	Component of rotor resultant force acting along X-axis
g	Acceleration due to gravity
h	Vertical distance between the helicopter center of gravity and the rotor hub
H	Drag force of the rotor in the tip-path plane
H.P.	Horsepower
I	Moment of inertia of blade mass about flapping hinge
J	Advance ratio of shrouded propeller
J_o	Advance ratio of shrouded propeller where the thrust goes to zero; Moment of inertia of body about its center of gravity
K_T	Thrust coefficient of shrouded propeller
K_{T_o}	Static thrust coefficient of shrouded propeller
l_t	Distance between the helicopter center of gravity and the shroud rotation axis
M_f	Pitching moment of fuselage
M_o	Thrust moment about blade flapping hinge

M_P	Rotor hub moment due to hinge restraint
M_q	Rotor damping with respect to pitch
M_t	Pitching moment of tail shroud
M_V	Rotor damping with respect to forward speed
n	Rotational speed of tail propeller
N_t	Force normal to tail shroud
P	Period of helicopter oscillations
q	Angular pitching velocity; dynamic pressure
q_v	Dynamic pressure in rotor downwash
Q	Torque
R	Rotor blade radius; Routh's discriminant
S	Area
S_w	Area of wing
t	Taper ratio of rotor blade; time
T	Thrust
T_t	Thrust of tail shrouded propeller
v_a	Axial velocity ratio
v_i	Induced velocity normal to the tip-path plane
v_o	Induced velocity at the rotor center
V	Forward velocity of the helicopter
V_t	Freestream velocity at the tail shroud
V_T	Rotor tip speed
W	Gross weight of the helicopter
x	Non-dimensional blade radius
$\overline{\alpha}$	Mean blade angle of attack
α_o	Section angle of attack

α_r	Angle of attack of the tip-path plane
α_w	Angle of attack of the wing
γ	Effective mass number
γ'	Lock Number
δ_o	Value of c_{d_o} at c_l equal to zero
δ_r	Tail shroud angular deflection in yaw
δ_t	Tail shroud angular deflection in pitch
δ_3	Angle of skew of flapping hinge
θ_R	Blade pitch angle
θ_T	Blade twist
θ_y	Tip-path plane pitch angle with respect to the horizontal
μ	Inplane velocity ratio at tip-path plane
ρ	Mass density of air
τ	Lift distribution correction factor
σ	Rotor solidity; air density ratio
ϕ_c	Angle between flight path and horizontal
ϕ_t	Pitch angular deflection of tail shroud in hovering equilibrium
Ω	Rotational velocity of rotor

SUMMARY

A small helicopter of unique configuration is proposed in this report, which should reduce the stability and control problems of conventional designs. At present, attempts to produce a helicopter which will compete in the private plane market have failed. These rotorcraft have sacrificed true helicopter operation in an effort to reduce cost, or they have simply modified conventional designs with no improvement in stability and control. A successful design should be one that is simple to fly, inexpensive to operate, and competitive in the light-plane field.

The proposed design incorporates two single-bladed rotors, laterally displaced and counter-rotating. A shrouded propeller is used on the tail of the machine for a control force in hovering flight, thus eliminating the necessity of cyclic pitch control to the rotor system. The laterally displaced rotors are supported on the ends of stub wings. These wings have the disadvantage of producing vertical drag in hovering flight, but this is seen to be offset by the advantage of reducing the power required in forward flight. Since the wing unloads the rotors, it also reduces the problems of asymmetric flow through the rotor at forward velocities.

A performance analysis shows that the helicopter will meet the requirement of acceptibility in the private plane field. The helicopter has a hovering ceiling of 3,200 feet out of ground effect and over 8,000 feet in ground effect. Thus, operation at normal altitudes is satisfactory and operation from high terrain is feasible. The power required

versus forward velocity gives a cruising speed of 70 knots while utilizing slightly over 50 per cent of power available. The helicopter has adequate fuel to operate at cruise for 2 hours with a 30 minute reserve.

The hovering stability analysis used conventional helicopter theory, taking into consideration the loss of efficiency due to the single-bladed rotor and counter-weight. These losses were seen to be tolerable when compared with the benefits derived from the blade with its very low Lock Number and its high energy of rotation. The effects of the shrouded tail propeller were also taken into consideration in the equations of motion of the hovering helicopter. The solution of these stability equations showed the helicopter to be very stable in hovering flight. It was found that the phugoidal oscillations were very long and lightly damped which presents no control problems.

It is concluded that the design is feasible, that the performance is adequate, and that the stability is exceptional. The simple control system and construction should enable the machine to be built for reasonable costs.

CHAPTER I

INTRODUCTION

Because of its versatility of operation, the helicopter has definitely established its place in the aviation picture. The increased mobility offered by the helicopter is causing radical changes in the present military organization, and the proven reliability of rotorcraft is making its use in civilian transportation commonplace. At present, however, helicopters are expensive and difficult to fly, and consequently they have not found a place in the private plane market. Modern advances in automatic stabilization and rigid rotor systems are making rotorcraft easier for the pilot to handle, but the expense increases with the complexity of these systems.

This paper will be concerned with the investigation of a design which should more closely meet the requirements of the light aircraft field. The configuration utilizes two main rotors mounted on stub wings with a shrouded propeller mounted on the tail of the fuselage. The counter-rotating main rotors eliminate counter-torque problems, and the use of the shrouded tail propeller as a control force in hover and forward flight eliminates the requirement for a complicated rotor head capable of cyclic pitch input to the rotor blades.

The proposed configuration is the unique feature of this report; however, to show the advantages of this design in the light-plane field, a detailed preliminary design of a feasible machine will be performed. Since the primary goal of the prototype helicopter will be safe operation

in hovering flight, the scope of this paper will be reduced to a hovering stability and control analysis. The performance required to show the general characteristics of the helicopter will be given. For the stability analysis, the techniques used for conventional helicopters will be employed where appropriate as outlined by Payne. Emphasis will be placed on those areas where the design is unique or where the parameters deviate from the conventional.

CHAPTER II

SURVEY OF POPULAR CONFIGURATIONS

There is today a market for a safe helicopter that can be easily flown and that can be cheaply built and maintained. The great impetus in the industry is for heavy military pay-loads and safe commercial passenger carriers. The helicopter is becoming more perfected every day, due to the demanding requirements of these two primary users. However, a small helicopter has not been produced which can compete in the private plane market. Attempts in this field so far have led to several new configurations. These will be discussed, and some of the characteristics of other configurations will be pointed out to show how they are not applicable to the private helicopter field.

The most extensively tried design is the gyrocopter, which is, in its simplest form, an autogyro without wings and is characterized by the fact that no power is delivered to the rotor. These machines are incapable of hovering flight or flight in any direction other than forward, consequently the main features of the helicopter are lost. Jump take-offs can be made with some gyrocopters; however, vertical flight cannot be sustained. Small helicopters with jets on the tips of the rotors have been flown successfully, but additional problems have arisen which have undermined their acceptability. The primary trouble with this design has been the high rate of fuel consumption and resulting short range. These two designs have both eliminated torque in the rotor mast and are simplified in that no counter-torque system is required. There

have also appeared several small conventional helicopters (single main rotor and counter-torque tail rotor), but the complexities of the control system and rotor head unfortunately are not decreased with the size of the craft. The hovering stability of a conventional helicopter is still a problem which requires considerable pilot experience for proficiency in hovering flight.

Counter-torque itself is not an insurmountable problem by any means. The systems used in conventional helicopters are, however, susceptible to high frequency vibrations, and control difficulties are often disastrous with counter-torque rotor failure. Counter-torque tail rotors in the future may be eliminated by the use of turbine engines with vectored exhaust thrust; at present the cost of turbine engines is such that the goal of an inexpensive machine cannot be realized using these engines.

Counter-torque problems can also be alleviated by using two counter-rotating main rotors. The tandem helicopter (two main rotors, one mounted fore and one aft on the fuselage) is a popular configuration and is used extensively by several of the larger helicopter companies in the United States. Control complexities are, unfortunately, a problem in this design and a small tandem helicopter would be impractical. Co-axial counter-rotating rotors offer a workable machine, but the co-axial drive and rotor heads are difficult to make and consequently very expensive. Two laterally mounted rotors rotating in opposite directions also eliminate the necessity for a counter-torque rotor. Designs of this configuration so far have not eliminated the problems of cost and complex controls encountered in present designs. Since the design under investi-

gation in this paper utilizes laterally disposed rotors, elaboration on this configuration will be in order.

Historically, one of the first successful designs used this lateral rotor configuration. The German Focke-Achgelis built in 1937 set an endurance record, and was thought to be a great step forward in helicopter advancement (1)*. The bulky lateral rotor supports were a drawback to the design, and future developments of the configuration were stopped. The design utilized differential collective for roll control and differential cyclic pitch for yaw control. This control system more than doubled the complications of the present conventional design. The Kaman HOK-1 Navy helicopter today uses laterally disposed rotors with the blades intermeshing "egg-beater" fashion (2). This is a successful production model which uses a unique pitch change system incorporating controllable servo flaps on the blades which twist the blades to the desired pitch setting. Again, control linkage and rotor structure make this technique cumbersome for a "simple" machine. The use of laterally disposed rotors as they appear in the design proposed in this paper should capitalize on the benefits of this configuration and minimize the drawbacks of the installation.

In summary, most emphasis to date has been placed on gyrocopters in an attempt to provide a 'helicopter' which will compete in the private plane market. As has been pointed out, however, the gyrocopter is not a helicopter. It can utilize the advantage of a jump take-off and short field operation, but it cannot operate at zero forward velocity. The modern popular helicopter configurations with their refinements are

---

*Refers to items in "Literature Cited" section.

highly successful machines, but in general, these configurations are not compatible with low cost construction and operation.

CHAPTER III

PRELIMINARY DESIGN

Configuration

The design proposed in this paper is a preliminary step in the development of a helicopter which should be easy to operate, comparatively cheap to build and maintain, and one having better stability than the conventional helicopter. No single component of this design is unique, nor is the proposed construction different from that incorporated in modern light aircraft and sailplanes. The design encompasses the use of two lifting rotors mounted near the tips of a small wing (see Appendix I). These rotors will be free to flap on the rotor mast and will have control linkage for collective pitch change. The rotors will each have a single blade and counter-weight. This type of blade has a reduced coning angle and a very low Lock Number, which is associated with a "heavy" blade. A shrouded propeller mounted at the tail of the fuselage will be capable of being rotated up and down and to the right and left. The entire system (two main rotors and tail propeller) will be operated at a constant speed.

Control of the helicopter will be maintained by the use of cockpit controls exactly like the conventional helicopter. The collective pitch stick will have a handgrip throttle and will control the vertical flight of the machine by applying collective pitch control uniformly to the two main rotors. The conventional cyclic pitch stick will pitch the nose of the helicopter up and down by rotating the shrouded tail up and

down and will provide roll control by applying differential collective pitch to the main rotors with lateral motion of the stick. Yaw control will be maintained with foot pedals which turn the shrouded propeller to the right and left.

The shrouded propeller will produce the control forces necessary in hovering flight for pitch and yaw. This tail thrust will be utilized for forward thrust in the lower velocity flight range, and at higher velocities when the thrust goes to zero the shroud system will still provide control like a conventional aircraft tail section. The stub wings will support the main rotors, and in forward flight the wings will unload the rotors reducing the problems of asymmetric flow relative to the rotor blades. The wing has a 50 per cent chord, full-span flap which deflects 60 degrees in hovering flight to reduce vertical drag.

Design Requirements

Although the helicopter configuration is the main feature of this paper, the full realization of the advantages of this configuration cannot be gained without a detailed design of a machine meeting the requirements of the light-plane market. Consequently, the design of a single place version of the rotorcraft will be elaborated upon and will necessarily be an important part of this paper. Construction will not be analyzed or dealt with, except where weight estimates are essential in the determination of the performance parameters. As with conventional aircraft, weight is definitely a problem and the use of modern construction techniques employed in wooden home-built type aircraft and sailplanes should be most appropriate.

In a preliminary design of this nature the most important goal is

safe operation in hovering flight. The following design requirements are thus proposed in an attempt to meet this goal and to have a machine efficient enough in its range of operation to be practical:

1. Hover in a 20 knot cross-wind.

2. Control sufficient to give acceleration in pitch and yaw of 20 degrees per second per second in hover.

3. Twelve degrees down flapping of the main rotors.

4. Tail shroud angular deflections of not more than 30 degrees.

5. Cruising flight speed of at least 65 knots.

6. Two hours flight endurance with a 30 minute fuel reserve.

In the performance calculations of the single-bladed rotor, a 20 per cent increase in the induced power required will be included. This should give a conservative estimate in the performance of the blade, considering the loss of efficiency associated with the strong tip vortex of the single blade. In multi-bladed rotors delivering the same thrust, the tip vortices will be weaker and spaced more closely together in the cylindrical tip wake, thus reducing induced power losses. Other than this consideration, standard rotor analysis will be used.

Selection and Determination of Governing Parameters

The first requirement in the design will be the estimation of the gross weight. This will be covered in the next chapter, and from the breakdown given in Appendix II the gross weight is estimated to be 850 pounds. The disc loading for the rotor system will be 1.5 pounds per square foot. This will be less than the average which is given by Nikolsky to be from 2.5 to 3.5 pounds per square foot (3). The lighter disc loading will reduce the structural loading on the blades and will

give a lower rate of vertical descent in autorotation, as this is proportional to the square root of the disc loading. The induced velocity in hover will also be reduced making operation over dusty soil safer.

With these two values the total required disc area is found to be 566 square feet, or one-half of this will be the swept area of each rotor. This rotor disc area of 283 square feet thus gives each rotor a radius of 9.5 feet. The rotor tip speed is selected to be 600 feet per second, which gives a rotor angular velocity, Ω , of 63.2 radians per second. The rotor blade counter-weight will be placed on an arm equal to one-half the blade radius.

The main rotors will be counter-rotating, such that the outboard movement of each rotor is aft and phased such that the blade of one rotor and the counter-weight of the other come together on a line between the rotor masts. This requires the rotor masts to be 14.25 feet apart, and for clearance the masts will be spaced 14.5 feet apart. Since the masts will be mounted on the tips of the wing this also will be the wing span. The rotor masts will be high enough to allow for 12 degrees of blade down-flapping and the tail shroud will be so placed that the down-flapping blades will not interfere with its operation.

With a pod-shaped fuselage adequate to house the pilot and engine the overall dimensions of the machine are thus determined.

Component Design Analysis

Main Rotor.--The lightly loaded main rotors with their single blades have the advantage of being a high energy system which eliminates some of the criticality of control application by the pilot during autorotation. Benefits are also derived from this blade in that it has an apparent

"heaviness" which reduces the coning angle of the blade and the problems associated with coning.

The NACA 0015 airfoil section will be used on the constant chord, untwisted blade. To find the chord required for the blade, the coefficient of thrust must be determined. Using the equation (4)

$$C_T = \frac{W/2}{\rho \pi \Omega^2 R^4} \qquad \text{(III-1)}$$

the coefficient of thrust was found to be 0.00175. (One-half gross weight is used in the equation since two rotors support the machine.) With a mean blade lift coefficient, $\bar{C}_L$, in hover of 0.45, from (5)

$$\bar{C}_L = \frac{6C_T}{\sigma} \qquad \text{(III-2)}$$

the blade solidity, σ, was found to be 0.0233. And since the solidity if defined by (6)

$$\sigma = \frac{b\,c}{\pi R} \qquad \text{(III-3)}$$

where b is the number of blades, the blade chord, c, can be determined and was found to be 8.35 inches. All of the blade dimensions are now known.

In order to determine the moment of inertia of the main rotor blades, a structural design must be made and is given in Appendix III. The blade structure must be kept simple and inexpensive if the machine as a whole is to be so classified. The blade is to have a one-piece stainless steel tube spar, which is also the counter-weight arm. Plywood

ribs will be cemented to this spar using epoxy resin glue; the blade will be plywood covered and finished with fabric and dope. The center of gravity of the blade will be at the quarter chord. The main spar will also be located at the quarter chord, and this will be the feathering axis of the blade. For the symmetrical airfoil section used, the moment coefficient is zero at the aerodynamic center. Thus, with the chordwise center of gravity, the feathering axis, and the aerodynamic center all on a coincident axis and with zero pitching moment about this axis, the blade will have good control characteristics without coupled bending and torsion assuming good blade bending rigidity.

The blade moment of inertia is 168.54 slug-feet squared with a total weight of 35.25 pounds. The Lock Number of the blade which is the relationship between the air forces and the mass forces acting on the blade is defined by (7)

$$\gamma = \frac{c\rho\, aR^4}{I} \qquad \text{(III-4)}$$

and is equal to 0.5. Normal blade Lock Numbers range from 8 to 15 with an infinitely heavy blade having a Lock Number of zero (8). Since damping in pitch of the rotor is inversely proportional to the Lock Number or blade mass factor, this is a very desirable pitch stabilizing factor (9).

In hovering flight the blade mean angle of attack $\overline{\alpha}$ will be equal to

$$\overline{\alpha} = \frac{2C_T}{ab\sigma_3} \approx \frac{6C_T}{a\,\sigma} \qquad \text{(III-5)}$$

which from Equation (III-2) is seen to be

$$\overline{\alpha} \approx \frac{\overline{C}_L}{a} \qquad \text{(III-6)}$$

where a is the slope of the lift-curve, $\frac{dC_L}{d\alpha}$. The mean blade angle of attack in hover is found to be equal to 0.0717. From unpublished works of Castles it is given that

$$\overline{\alpha} = A_o - \sqrt{C_T} \qquad \text{(III-7)}$$

where A_o is the collective pitch angle, and this pitch setting in hover is found to be 6.51 degrees.

The blade coning angle in hovering flight is found from the relationship (10)

$$M_o \approx - a_o I \Omega^2 \qquad \text{(III-8)}$$

where M_o is the blade thrust moment about the flapping hinge.

This relationship is a good approximation since, for the flapping blade the summation of moments about the flapping hinge must be zero, and the steady part of the blade inertia moment about the flapping hinge in hover is largely the centrifugal moment $- a_o I \Omega^2$. The coning angle in hovering flight for the single-bladed rotors was found to be 0.258 degrees.

Tail Propeller and Shroud.--A shrouded propeller was selected for this design because of its increased thrust in static operation over a free propeller of the same diameter (11). It is again pointed out that a force is needed in static operation (hovering flight) to provide the

forces necessary to control the machine at zero forward velocity if the rotors are to be simplified by having no cyclic control. Conventional tail surfaces, for instance, would be ineffective with zero dynamic pressure; the gyrocopter, on the other hand, can use the conventional tail section because it is incapable of hovering flight.

For purposes of this report the shrouded tail propeller will be considered as a unit, and the shroud curvature and the propeller blade dimensions will not be specified. A literature search has shown that a shroud of the overall dimensions specified in this design is practical, and satisfactory operation can be obtained using a two-bladed propeller. A horizontal and vertical fin will be placed in the shroud exit to increase the overall efficiency by reducing the rotation of the exit flow (12). In the event of tail propeller failure, these surfaces will supplement the shroud in acting as a conventional tail surface; hovering flight capability will be lost, but a conventional aircraft landing can safely be made with such a failure.

The dimensions of the shroud compatable with structural limitations, design clearance, and efficient operation were found to be: diameter 3.0 feet, shroud chord (length) 2.0 feet, and exit area 7.06 square feet. The thrust of the system will be that required to meet the most stringent of the two requirements: first, hover in 20 knot cross-wind and second, acceleration in pitch and yaw of 20 degrees per second per second. These requirements are to be met using a shroud angular deflection of no more than 30 degrees.

For the first requirement, a side drag of 36.1 pounds was estimated in the 20 knot cross-wind, acting 38.5 inches aft of the center of

gravity. The shroud thrust required for this condition was found to be 27.8 pounds (see Figure 1). For the second requirement it is estimated in Appendix IV that the moment of inertia of the machine in yaw is 555 slug-feet squared, and in pitch is 202 slug-feet squared. For equal shroud angular deflections vertically and laterally, the case of yaw is seen to be most demanding. From the simple relationship that the turning moment is equal to the moment of inertia times the angular acceleration,

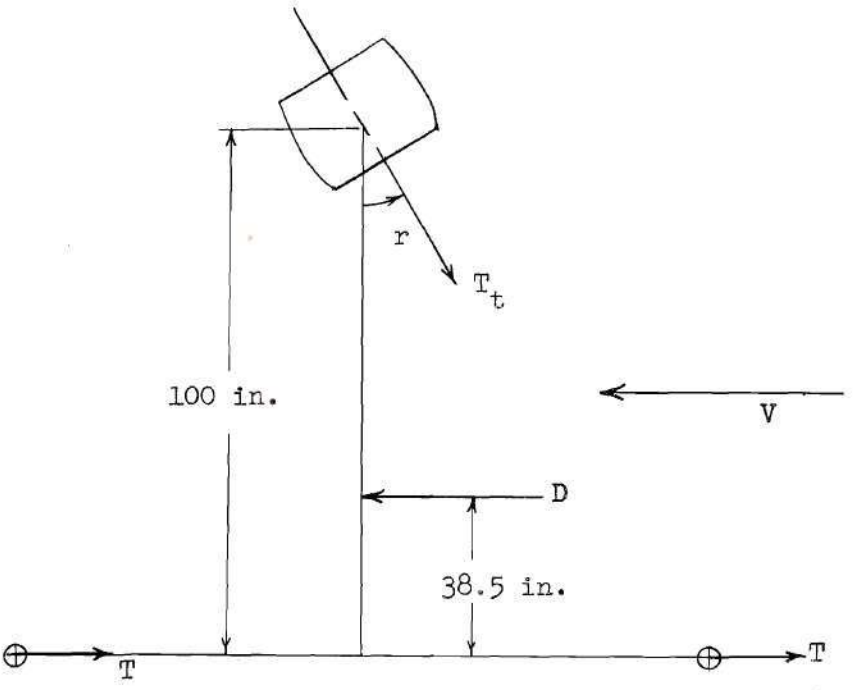

Figure 1. Tail Thrust Required in Cross-Wind

the shroud thrust for this condition was found to be 46.5 pounds. This is seen to be the critical requirement for the tail shrouded propeller, and will thus be the thrust required of the system.

For this thrust and from the given shroud area, the disc loading of the shroud is 6.58 pounds per square foot. Payne (13) gives for this

disc loading and a mean blade lift coefficient of 0.5, a power required of 3.5 horsepower with a blade solidity of 0.15. From Equation (III-3) this solidity will give a blade chord of 4.24 inches. With this chord and a propeller diameter of 36 inches, there should be no structural problems in blade fabrication.

Wings.--The purpose of the wing in this design is twofold. First, it serves as a "fairing" for the lateral rotor support, and second, it unloads the rotors in forward flight. Any fixed lifting surface on a helicopter is a problem, in that the transition from hover to forward flight must be controllable at least, but for acceptability the transition must be smooth. The area of the surfaces in the rotor downwash must also be minimized to reduce vertical drag in hovering flight.

From airfoil theory it is known that for airfoil sections with a thickness to chord ratio of greater than 15 per cent the stall is more gentle. The stall of these thick airfoils is characterized by a flatter lift curve at maximum lift, resulting in a gentle stall (14). This gives a smoother transition from the unstalled to the stalled condition, than does the thin airfoil with its characteristic abrupt stall. The NACA 6421 airfoil will be used on the wing. It displays the desired stall characteristics (15), and the large airfoil thickness allows adequate room for housing the rotor drive in the wing. The thick airfoil will also be more favorable from a structural standpoint, in that the machine will be "held up by the wing tips" in hovering flight.

The problem of vertical drag will be reduced somewhat by the low disc loading of the rotors, which reduces the dynamic pressure in the downwash. To further alleviate the problem the wing will incorporate a

50 per cent chord, full-span flap capable of being deflected 60 degrees. It will be shown later in this paper that the vertical drag contributes less than 5 per cent to the hovering thrust, which is tolerable.

It has already been pointed out that a wing span of 14.5 feet will be required. A 30-inch chord will give the wing an aspect ratio of 5.8. A wing structural analysis will not be performed, since no difficulties are anticipated. A lift strut can be utilized to carry some of the wing load if it is deemed necessary. The wing tip configuration will depend somewhat on the drive used for the main rotors. If a bulky or awkward gear box is used at the rotor mast, a fairing resembling a wing tip tank will make a more efficient installation.

Fuselage.--The fuselage will not be elaborated upon, since it is small and simple. A sailplane pod-type fuselage will be used -- there will be no provision for a payload in this small prototype. The cockpit will be fitted with conventional helicopter controls and only those instruments and accessories consistent with safe operation. The engine will be mounted behind the pilot and fitted with ducting necessary for cooling. The aft section of the fuselage will have to house the tail propeller drive and the control linkage to the shrouded propeller, and will have to be rigid enough to take the loads imposed by the tail shroud.

Landing Gear.--The lightness of the machine will simplify the landing gear requirements. A skid under the nose section of the fuselage will serve as a runner, exactly as that used on a sailplane. A single wheel located at the center of gravity will facilitate ground handling. Outrigger struts on the wing tips will prevent the machine from resting in an awkward wing low attitude. A "stinger" skid will be used on the rear

of the fuselage to prevent banging the tail shroud into the ground on tail-low approaches and in ground handling.

This gear might seem oversimplified; however, it is pointed out that light helicopters "taxi" in the air and not on their landing gear.

CHAPTER IV

WEIGHT AND BALANCE

The weight and balance data are given in Appendix II. Lightness will be strived for in all parts of the structure. The requirement on the center of gravity location is that it be made to lie longitudinally at the rotor mast axis and that its travel be as small as possible. Since the fuel is the only expendable load, it has been located as close to the required longitudinal station as possible. The extremes of the fuel load produce slightly less than a quarter of an inch travel in the center of gravity location. This small travel will be of negligible consequence, due to the power available in pitch from the shrouded propeller.

Weight estimates are based on wood and fabric construction, with steel tubing used in high stress areas. The engine is a McCulloch drone engine, rated at 72 horsepower and weighing approximately 79 pounds. It has a fuel consumption of 4.5 gallons per hour. The endurance will require a fuel load of 72 pounds.

CHAPTER V

PERFORMANCE

A performance analysis will be made of the proposed helicopter to more generally define the flight characteristics of the machine.

For the proposed design the 72 horsepower McCulloch Drone Engine has numerous advantages. First, the engine is light, has a good power-to-weight ratio, and can be readily obtained for a very reasonable price (16). The two-cycle engine is air cooled and can be mounted in the vertical position with very minor modification. Since the engine will be operated at a constant speed near peak rpm, the disadvantage of the two-cycle engine's poor idling performance will not be manifest. The available horsepower will be taken as 90 per cent of rated; the 10 per cent reduction will cover cooling and gear losses. Thus, it will be assumed that the available horsepower is 64.8.

Power Required in Hovering Flight

To determine the horsepower required in hovering flight (disregarding the benefits of ground effect), the vertical drag is computed in Appendix V based on the following assumptions:

1. The wake has fully contracted and the downwash has reached the ultimate velocity of twice the induced velocity at the rotor plane.

2. The wing flap is lowered 60 degrees.

3. The wing and fuselage in the downwash has a coefficient of drag of 1.0.

4. The total surface area in downwash is equal to the wing pro-

jected area with flaps lowered 60 degrees.

The 41.0 pounds of vertical drag thus determined make the thrust required 891 pounds. Using appropriate tabulated performance parameters (17) and assuming that the induced torque to be increased 20 per cent over normal rotor configurations, the horsepower required to hover, including the 3.5 horsepower for the tail propeller, is 57.9. This power required includes a 5 per cent loss in the rotor drive system, and gives a 12 per cent excess power available in hover out of ground effect (see Appendix VI). The increased power required factor for the single-bladed rotor, as explained earlier in this paper, was determined by Professor Castles in unpublished works. The blade tip drag was considered negligible in this case and the tip stall effects were not a factor.

Hovering Ceiling

To determine the hovering ceiling the horsepower available is assumed to vary as the air density. More specific data is not available on the engine, and this should be a conservative ratio when the benefits derived from the decreased ambient temperature with increased altitude are considered. In Appendix VII the hovering ceiling was found to be 3200 feet, which indicates very satisfactory operation at sea level. When operation in the ground cushion is considered with a 20 per cent reduction in power required (18), the hovering ceiling in ground effect is over 8,000 feet. Therefore, the operation of the machine from high terrain is also certainly adequate.

Power Required Versus Forward Speed

The horsepower required versus the forward velocity will next be determined for sea level operation. A drag analysis of the helicopter

will first have to be made for forward flight; this is presented in detail in Appendix VIII. Hoerner was used as a basis for the component drag estimation, and a 10 per cent increase was used to insure a conservative estimate. The induced drag at 65 knots was determined, and it will be assumed that the induced drag will have this same ratio to the total drag throughout the flight range. The significance of this assumption will become apparent when the iterative process required to determine the helicopter pitch angle is investigated in the power required calculations in Appendix IX. Again, conventional helicopter analysis will be used with the parasite drag, commonly termed fuselage drag, D_F, being the resultant of the tail shrouded propeller thrust and the parasite and induced drag. The thrust from the shrouded propeller was determined from the non-dimensionalized ratios given in Appendix X. It will be assumed that the power required for the tail propeller will vary as the thrust, since it is operating at a constant pitch and velocity.

The first step in calculating the horsepower required versus forward speed is to determine the incidence of the wing. Since the cruise speed desired is approximately 65 knots, the wing will be set at its best lift to drag ratio at this velocity. The lift coefficient is 0.4 at this optimum ratio, and with the other wing parameters fixed the lift generated is 208.6 pounds. This lift unloads the rotors and is subtracted from the gross weight to give the effective weight. The drag force, D_F, is found from Figure 15 to be 36.6 pounds. Thus using the performance estimation proposed by Professor Castles, the pitch angle Θ_y can be calculated from

$$\tan \Theta_y = - \frac{D_f \cos \phi_c + F_X \cos \Theta_y}{W - D_f \sin \phi_c + F_X \sin \Theta_y} \qquad \text{(V-1)}$$

where F_X is the rotor force in the X direction (see Figure 2 below).

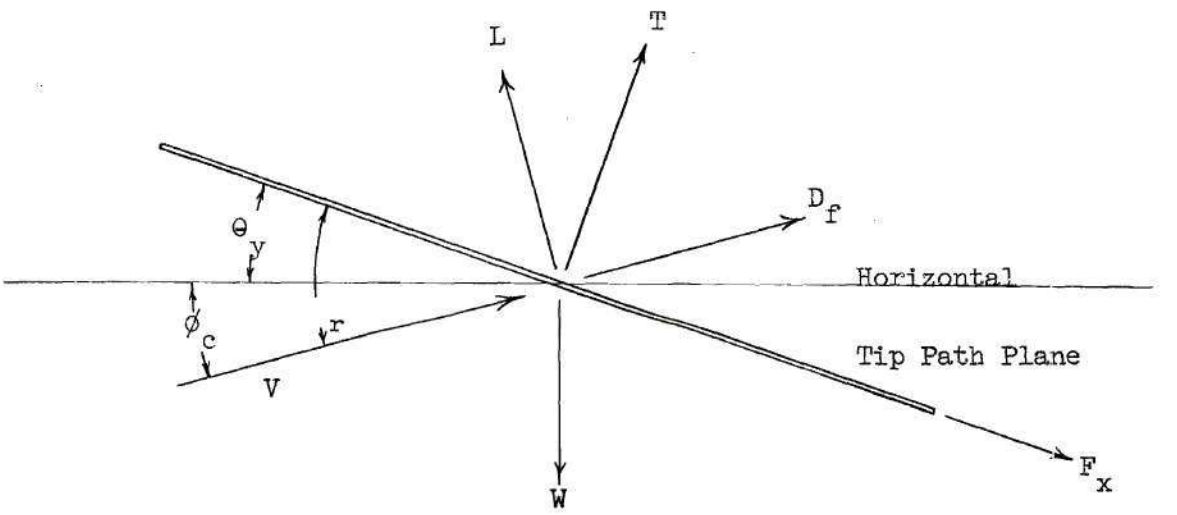

Figure 2. Forces Acting on the Rotor Hub

For horizontal flight, the case under consideration, ϕ_c is equal to zero. For small pitch angles the equation

$$\tan \Theta_y \approx - \frac{D_f \cos \phi_c}{W - D_f \sin \phi_c} \qquad \text{(V-2)}$$

can be used as a first approximation for a second iteration in Equation (V-1). Using these equations the pitch angle of the helicopter was found to be - 3.47° at 65 knots. The angle of attack of the wing was found from data in NACA Technical Report Number 460 and the equation (19)

$$\alpha_w = \alpha_o + \frac{C_L}{\pi A}(1 + \tau) \qquad \text{(V-3)}$$

where the non-elliptic lift distribution correction factor, τ, is equal to 0.16 for an aspect ratio of 5.8. The angle of attack thus corrected for a three-dimensional airfoil is 2.46°. This, in conjunction with the already determined pitch attitude, gives the required incidence of the wing to be 5.93°. At cruising velocity it is assumed that the downwash does not affect the freestream flow at the wing, though its effect will require an increase in the angle of incidence.

The horsepower required for various forward velocities can now be found. Using the iterative process outlined above for Θ_y, it must be realized that the lift will vary directly with this pitch attitude angle. The rotor angle of attack, α_r, can be found from

$$\alpha_r = \phi_c + \Theta_y \qquad \text{(V-4)}$$

With this angle the inplane velocity ratio, μ, can be found from the relationship

$$\mu = \frac{V \cos \alpha_r}{\Omega R} \qquad \text{(V-5)}$$

and the freestream inflow velocity ratio can be found using the equation

$$v_a = \frac{V \sin \alpha_r}{\Omega R} \qquad \text{(V-6)}$$

Using Equation (III-1) as a first approximation, the coefficient of thrust can be found from the equation

$$C_T = \frac{W - D_f \sin \phi_c + F_X \sin \theta_y}{\rho \pi \Omega^2 R^4 \cos \theta_y} \qquad (V\text{-}7)$$

With these parameters the remaining performance parameters of the rotor can be determined and the horsepower required for a given velocity can be calculated. These data are presented in Table 8, Appendix IX. It was assumed that the lift curve slope, a, is equal to 2π. In the determination of the rotor X-force due to the profile drag, the profile drag coefficient, c_{d_o}, is approximated by the first two terms of the even power series in the blade-element lift coefficient, c_l, i.e. (20)

$$c_{d_o} = \delta_o + \epsilon c_l^2 \qquad (V\text{-}8)$$

where δ_o and ϵ are assumed to have the typical values of 0.008.

CHAPTER VI

HOVERING STABILITY AND CONTROL

Introduction to Helicopter Hovering Stability

A body in space has six degrees of freedom, three linear velocities along the co-ordinate axes and three angular velocities about these axes. A conventional aircraft is capable of control in four of these modes, being incapable of flight along its vertical and lateral axes. A helicopter on the other hand, is capable of movement in all six modes. It is, however, assumed that lateral and longitudinal velocities are coupled with roll and pitch. Thus, the control requirements are reduced from six to four; these are pitch, roll, yaw, and vertical velocity. As has already been pointed out, the pilot's controls of the proposed design are exactly like those of the conventional helicopter. The required control power of the shroud for pitch and yaw has already been calculated. Since the vertical flight control will be simple collective pitch and roll control will be differential collective pitch to the two rotors, there will be no problem in getting the required control power. The delicate linkage adjustments and swashplate phasing for cyclic pitch input to the rotor system are thus eliminated, since no cyclic pitch is required.

It is the purpose of this paper to investigate the stability of the proposed design in hovering flight. In such an analysis it is common practice to reduce the degrees of freedom from the four mentioned to two. By the definition of hovering flight the vertical velocity is equal

to zero, and it is known that vertical motion does not affect the phugoidal oscillation (21). It is further assumed that the two coupled degrees of freedom of horizontal velocity and pitch are more important than the roll and the related lateral velocity.

Equations of Motion in Hovering Flight

The equations of motion for two degrees of freedom are

$$a_1\ddot{x} + b_1\dot{x} + c_1x + a_2\ddot{y} + b_2\dot{y} + c_2y = A_1\Theta \qquad \text{(VI-1)}$$

$$a_3\ddot{x} + b_3\dot{x} + c_3x + a_4\ddot{y} + b_4\dot{y} + c_4y = A_2\Theta \qquad \text{(VI-2)}$$

where x and y are the instantaneous co-ordinates of the system; the single and double dotted terms are the velocity and acceleration, respectively. The horizontal velocity will be $\dot{x}$ and the pitch angle between the fuselage datum and the horizontal will be y.

The static equations of the helicopter will be those as outlined by Payne, plus the contribution of the tail propeller and shroud. For terminology simplification the thrust from the two rotors will be considered as one thrust vector, and all other rotor forces will be summed for the two rotors, except where noted. Referring to Figure 3 on the following page it can be seen that the static equations are: first summing horizontal forces,

$$H\cos\Theta + D_f - T(B_1 - a_{1_s} - \Theta) - T_t\cos(\Theta - \phi_t + \delta_t) \qquad \text{(VI-3)}$$

$$- N_t\sin(\Theta - \phi + \delta_t) = 0$$

and summing moments about the center of gravity,

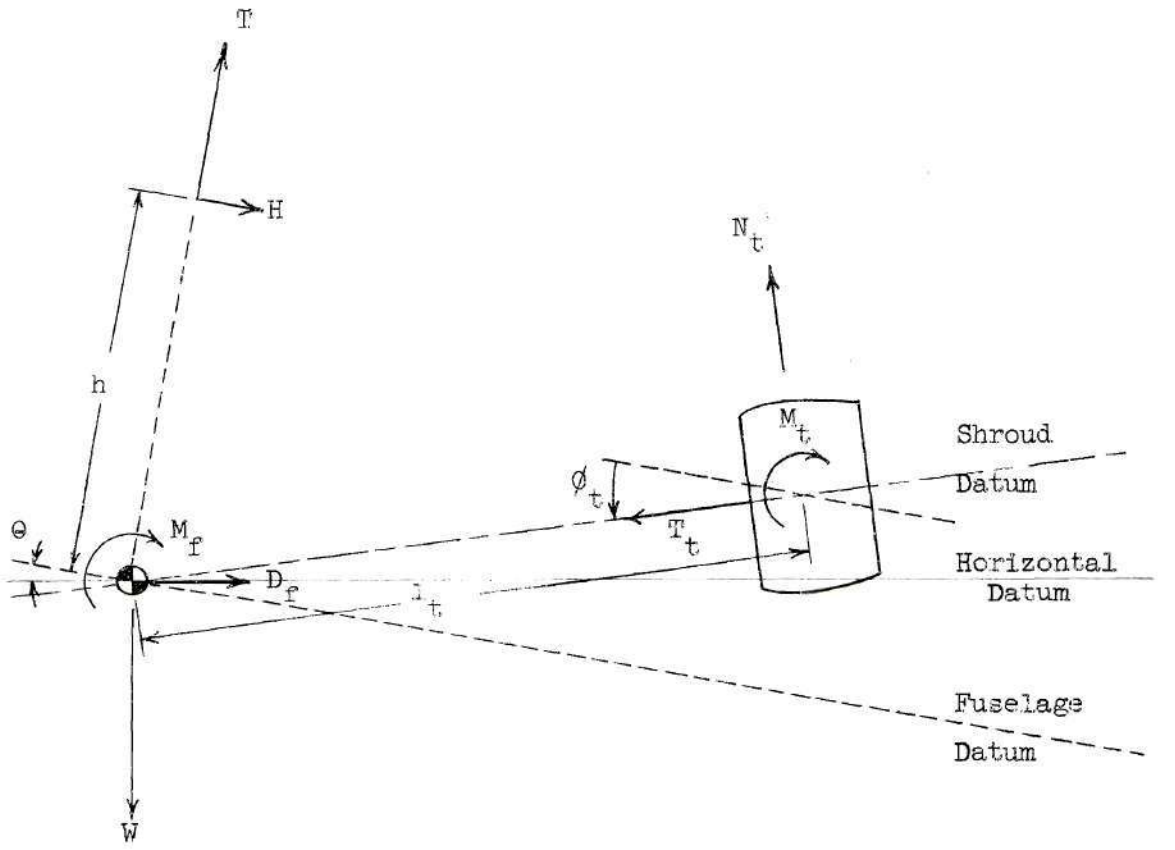

Figure 3. Forces Acting on the Helicopter

$$M_c + M_p - Th(B_1 - a_{1_s}) + H_h + M_t \qquad \text{(VI-4)}$$

$$- N_t l_t \cos \delta_t - T_t l_t \sin \delta_t = 0$$

The tail shroud angles are more clearly defined in Figure 4 where δ_t is the control input angular deflection and the angle ϕ_t is the fixed

angle of hovering equilibrium.

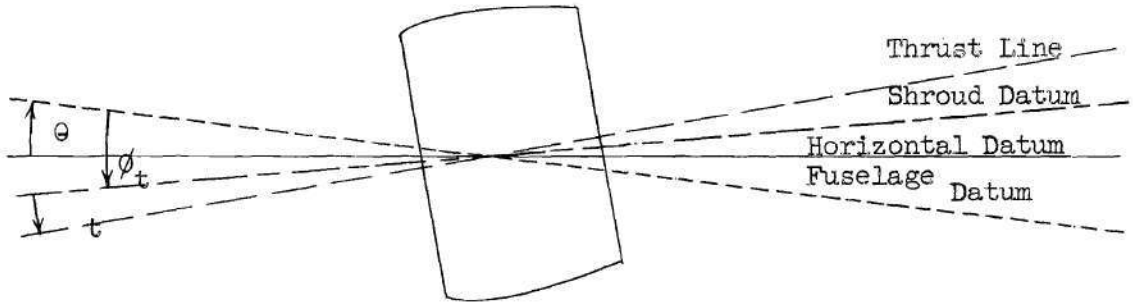

Figure 4. Tail Shroud Angles

For the hovering flight condition under consideration the following assumptions are made:

1. Small disturbances from equilibrium hovering flight.
2. The main rotor downwash does not appreciably affect the tail shroud.
3. The thrust acts normal to the tip path plane.
4. The center of gravity is on the rotor shaft axis.
5. The fuselage moment is equal to zero.
6. B_1 is equal to zero.
7. Control input to the tail, δ_t, is equal to zero and the stick is fixed.

In the static case a_{1_s} is also equal to zero, but in the dynamic case it will be a function of the angular velocity of pitch, $q = d\theta/dt$, and the rotor in-plane velocity $(V + hq)$, thus (22)

$$\Delta a_{1_s} = \frac{\partial a_{1_s}}{\partial V}(V - hq) - \frac{da'}{da_1}\frac{\partial a_{1_s}}{\partial q} q \qquad \text{(VI-5)}$$

The second term in Equation (VI-5) is due to the fact that in a pitching motion the thrust is not perpendicular to the tip path plane. It will be noted that the signs in Equation (VI-5) have been changed from those appearing in Payne. In the stability equations it was found that these changes had to be made to realize the damping due to rotor disc lag. Considering the effect of Δa_{1_s} and adding inertia terms, Equation (VI-3) becomes

$$\frac{W}{g}\frac{dV}{dt} - \frac{\partial T_t}{\partial V} V \cos(\Theta - \phi + \delta_t) - \frac{\partial N_t}{\partial V} V \sin(\Theta - \phi + \delta_t) \qquad \text{(VI-6)}$$

$$+ H \cos\Theta + D_f + T\Delta a_{1_s} + T\Theta - T_t \cos(\Theta - \phi + \delta_t) - N_t \sin(\Theta - \phi + \delta_t) = 0$$

Since the rotor is freely flapping with no hinge restraint and M_p is equal to zero, the moment equation can be written adding the inertia terms,

$$- I\frac{d^2\Theta}{dt^2} + Th\,\Delta a_{1_s} + Hh + l_t\frac{\partial M_t}{\partial V_t}\frac{d\Theta}{dt} \qquad \text{(VI-7)}$$

$$- l_t^2\frac{\partial N_t}{\partial V_t}\frac{d\Theta}{dt} + \frac{\partial M_t}{\partial \Theta}\Theta - l_t\frac{\partial N_t}{\partial \Theta}\Theta = 0$$

Equations (VI-6) and (VI-7) can be reduced and put in a simpler form when the assumptions listed are considered, and when the equations are divided throughout by the weight which is approximately equal to the thrust. These equations become respectively,

$$\frac{1}{g}\frac{dV}{dt} + \frac{V}{W}\left(\frac{\partial H}{\partial V} + \frac{\partial D_f}{\partial V}\right) + \theta + \frac{\partial a_{1_s}}{\partial V} V \qquad \text{(VI-8)}$$

$$- \left(\frac{da'}{da_1}\frac{\partial a_{1_s}}{\partial q} + \frac{\partial a_{1_s}}{\partial V} h\right)\frac{d\theta}{dt} - \frac{T_t}{W}\cos(\theta - \phi) = 0$$

$$- \frac{I}{Wh}\frac{d^2\theta}{dt^2} + \frac{V}{W}\frac{\partial H}{\partial V} + \frac{\partial a_{1_s}}{\partial V} V + \left[- \frac{da'}{da_1}\frac{\partial a_{1_s}}{\partial q} - \frac{\partial a_{1_s}}{\partial V} h \right. \qquad \text{(VI-9)}$$

$$\left. + \frac{l_t}{Wh}\left(\frac{\partial M_t}{\partial V_t} - l_t\frac{\partial N_t}{\partial V_t}\right)\right]\frac{d\theta}{dt} + \frac{1}{Wh}\left(\frac{\partial M_t}{\partial \theta} - l_t\frac{\partial N_t}{\partial \theta}\right)\theta = 0$$

For small disturbances from hovering equilibrium $\frac{\partial H}{\partial V}$ and $\frac{\partial D_f}{\partial V}$ are approximately equal to zero, thus the two equations can be further reduced to,

$$\frac{1}{g}\frac{dV}{dt} + \frac{\partial a_{1_s}}{\partial V} V - \left(\frac{da'}{da_1}\frac{\partial a_{1_s}}{\partial q} + \frac{\partial a_{1_s}}{\partial V} h\right)\frac{d\theta}{dt} \qquad \text{(VI-10)}$$

$$+ \theta - \frac{T_t}{W}\cos(\theta - \phi) = 0$$

$$- \frac{I}{Wh}\frac{d^2\theta}{dt^2} + \frac{\partial a_{1_s}}{\partial V} V + \left[- \frac{da'}{da_1}\frac{\partial a_{1_s}}{\partial q} - \frac{\partial a_{1_s}}{\partial V} h \right. \qquad \text{(VI-11)}$$

$$\left. + \frac{l_t}{Wh}\left(\frac{\partial M_t}{\partial V_t} - l_t\frac{\partial N_t}{\partial V_t}\right)\right]\frac{d\theta}{dt} + \frac{1}{Wh}\left(\frac{\partial M_t}{\partial \theta} - l_t\frac{\partial N_t}{\partial \theta}\right)\theta = 0$$

The two equations of motion, Equations (VI-1) and (VI-2), can be written in terms of V and θ as

$$a_1 \frac{dV}{dt} + b_1 V + c_1 x + a_2 \frac{d^2\theta}{dt^2} + b_2 \frac{d\theta}{dt} + c_2 \theta = A_1 \qquad \text{(VI-12)}$$

$$a_3 \frac{dV}{dt} + b_3 V + c_3 x + a_4 \frac{d^2\theta}{dt^2} + b_4 \frac{d\theta}{dt} + c_4 \theta = A_2 \qquad \text{(VI-13)}$$

Comparing Equations (VI-10) and (VI-11) to Equations (VI-12) and (VI-13) gives:

$$a_1 = \frac{1}{g}$$

$$b_1 = \frac{\partial a_{1_s}}{\partial V}$$

$$c_1 = 0$$

$$a_2 = 0$$

$$b_2 = -\left(\frac{da'}{da_1} \frac{\partial a_{1_s}}{\partial q} + \frac{\partial a_{1_s}}{\partial V} h\right)$$

$$c_2 = 1 - \frac{T_t}{W} \sin \phi$$

$$a_3 = 0$$

$$b_3 = \frac{\partial a_{1_s}}{\partial V}$$

$$c_3 = 0$$

$$a_4 = -\frac{I}{Wh}$$

$$b_4 = \left[-\frac{da'}{da_1} \frac{\partial a_{1_s}}{\partial q} - \frac{\partial a_{1_s}}{\partial V} h + \frac{l_t}{Wh}\left(\frac{\partial M_t}{\partial V_t} - l_t \frac{\partial N_t}{\partial V_t}\right)\right]$$

$$c_4 = \frac{1}{Wh}\left(\frac{\partial M_t}{\partial \theta} - l_t \frac{\partial N_t}{\partial \theta}\right)$$

If the solutions of Equations (VI-12) and (VI-13) are assumed to

be of the form

$$x = x_o e^{\lambda t} \tag{VI-14}$$

$$\theta = \theta_o e^{\lambda t} \tag{VI-15}$$

then the characteristic equation is

$$a\lambda^4 + b\lambda^3 + c\lambda^2 + d\lambda + e = 0 \tag{VI-16}$$

where

$$a = (a_1 a_4 - a_2 a_3)$$

$$b = (a_1 b_4 + b_1 a_4 - a_2 b_3 - b_2 a_3)$$

$$c = (a_1 c_4 + b_1 b_4 + c_1 a_4 - a_2 c_3 - b_2 b_3 - c_2 a_3)$$

$$d = (b_1 c_4 + c_1 b_4 - b_2 c_3 - c_2 b_3)$$

$$e = (c_1 c_4 - c_2 c_3)$$

The stability of Equation (VI-16) is defined by Routh's discriminant (23)

$$R = bcd - ad^2 - b^2 e \tag{VI-17}$$

There will be at least one unstable mode if $R < 0$; the coefficients b , c , d , and e must all be positive if the motion is stable and e must be positive for the condition of static stability.

Determination of the Stability Derivatives

Payne will again be used as a guide in determining the stability

derivatives. The single rotor parameters will be used in these calculations, since the individual blade behavior is the determining factor. Because the blades are counter-rotating the lateral forces will cancel and the other parameters, which govern the stability, will be in the same sense for the two rotors and will add.

Given the equation

$$a_{1_c} = - \frac{2q\gamma}{\Omega t_4} \qquad \text{(VI-18)}$$

for rotors having coincident control and hub orbits, which is the case in the proposed design, the stability derivative, $\frac{\partial a_{1_s}}{\partial q}$, is seen to be

$$\frac{\partial a_{1_s}}{\partial q} = - \frac{2\gamma}{\Omega} \qquad \text{(VI-19)}$$

where the taper integral t_4 is equal to 1.0 from the equation (24)

$$t_n = 4 \int_{x_1}^{x_2} (1 - t^* x) x^{n-1} \, dx \qquad \text{(VI-20)}$$

The blade taper, t^*, is equal to zero for the untapered rotor blade, and the integral is evaluated from zero to 1.0. The blade "inertia number", γ, is similar to the Lock Number, but inversely proportional to it, and is defined by (25)

$$\gamma = \frac{I}{\frac{1}{8} \rho R^4 ac} \qquad \text{(VI-21)}$$

and is equal to 15.95. Thus, the derivative $\frac{\partial a_{1_s}}{\partial q}$ is equal to - 0.505.

Due to the pitching velocity of the rotor, the rotor thrust cannot be assumed normal to the tip path plane; this is called Amer's effect. The derivative defining this effect is given by (26)

$$\frac{da'}{da_1} = 1 - \frac{t_2 \lambda_o}{2C_T} \qquad \text{(VI-22)}$$

where t_2 is found from Equation (VI-20) and the blade inflow ratio, λ_o, in hovering flight is

$$\lambda_o = \frac{v_o}{V_T} \qquad \text{(VI-23)}$$

The induced velocity v_o in hover is 17.84 feet per second, and the derivative $\frac{da'}{da_1}$ is equal to - 15.1. The final stability derivative of the main rotor is the change in tip path tilt back with velocity given by (27)

$$\frac{\partial a_{1_s}}{\partial V} = \frac{(2t_3 \Theta_R - 2t_4 \Theta_T - t_2 \lambda_o)}{V_T \left[t_4 + \frac{(c_k + t_4 \tan \delta_3)^2}{t_4} \right]} \qquad \text{(VI-24)}$$

$$+ \frac{\frac{t_3}{t_4} a_o (c_k + t_4 \tan \delta_3) + \frac{\partial \lambda_1 K}{\partial \mu} (c_k + t_4 \tan \delta_3)}{V_T \left[t_4 + \frac{(c_k + t_4 \tan \delta_3)^2}{t_4} \right]}$$

This equation reduces to a simpler form, due to the untwisted blade having no hinge restraint in flapping and having no delta angle in the flapping hinge. The reduced equation is

$$\frac{\partial a_{1_s}}{\partial V} = \frac{2t_3 \theta_R - t_2 \lambda_o}{V_T t_4} \qquad \text{(VI-25)}$$

and the derivative is equal to 0.000413. The stability parameters of the main rotors are thus determined.

The stability contribution of the tail shroud is not as clearly defined as that of the main rotors. In the material available on shrouded propellers (ducted fans), little information was available in the operating range of the stability analysis. Since this preliminary design did not warrant the time and expense of a wind tunnel analysis of the required shrouded propeller, the best reference had to be determined. The static coefficient of thrust for the shrouded propeller was calculated to be 0.087. The figures from a thesis by H. J. Allen, reproduced by Theodorsen (28), substantiate the fact that a shroud with this static coefficient can deliver thrust over the desired advance ratio range. The other desired parameters were not available, however. The complete data on the shrouded propeller in NACA Technical Note 3547, however, did give the desired parameters and will be used. In the case where this shroud is other than conservative, as compared with the available data, the parameters will be corrected to insure a conservative estimate.

In the literature the parameters of the shrouded propeller are presented for various advance ratios, J, defined by

$$J = \frac{V}{nd} \qquad \text{(VI-26)}$$

In the terminology of this paper the freestream velocity at the shroud will be designated V_t. This velocity for computing the normal force

and moment in a pitching disturbance from hovering flight will be the pitching angular velocity, q, times the tail length, l_t, (see Figure 5). Thus, for small disturbances from hovering flight the resulting advance ratio will necessarily be very small.

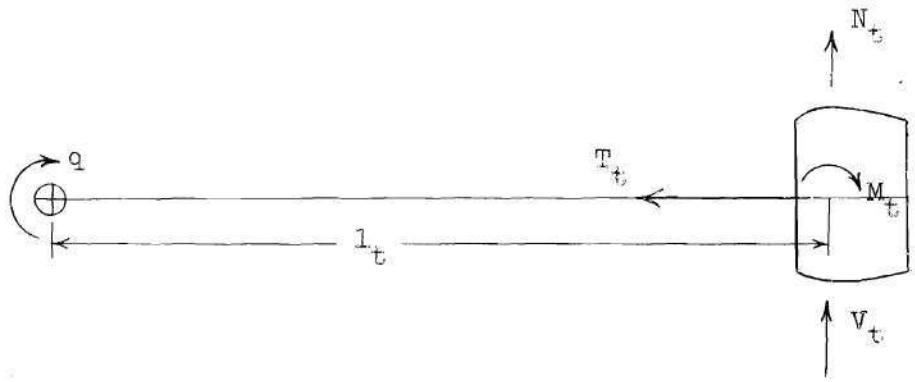

Figure 5. Tail Shroud Forces

The derivatives of the moment and normal force of the shroud, with respect to V_t, were found in Appendix X to be 0.53 and 0.70, respectively. The derivatives of the moment and normal force, with respect to the shroud angle of attack Θ, were found to be 7.24 and 47.3, respectively.

All of the derivatives are now evaluated and the coefficients of the characteristic Equation (VI-16) can be calculated, taking into account the contribution of the two rotors giving:

$$a = -\frac{2I}{Whg} = -0.0037$$

$$b = \frac{1}{g}\left[-\frac{da'}{da_1}\frac{\partial a_{1_s}}{\partial q} - \frac{\partial a_{1_s}}{\partial V}h + \frac{l_t}{Wh}\left(\frac{\partial M_t}{\partial V_t} - l_t\frac{\partial N_t}{\partial V_t}\right)\right] - \frac{\partial a_{1_s}}{\partial V}\frac{2I}{Wh}$$

$$= -0.2373$$

$$c = \frac{1}{Whg}\left(\frac{\partial M_t}{\partial \theta} - l_t \frac{\partial N_t}{\partial \theta}\right) + \frac{\partial a_{l_s}}{\partial V}\left[- \frac{da'}{da_l}\frac{\partial a_{l_s}}{\partial q} - \frac{\partial a_{l_s}}{\partial V} h + \frac{l_t}{Wh}\left(\frac{\partial M_t}{\partial V_t} - l_t \frac{\partial N_t}{\partial V_t}\right)\right] - \frac{\partial a_{l_s}}{\partial V}\left[- \frac{da'}{da_l}\frac{\partial a_{l_s}}{\partial q} - \frac{\partial a_{l_s}}{\partial V} h \right] = - 0.00437$$

$$d = \frac{1}{Wh}\frac{\partial a_{l_s}}{\partial V}\left(\frac{\partial M_t}{\partial \theta} - l_t \frac{\partial N_t}{\partial \theta}\right) - \frac{\partial a_{l_s}}{\partial V}\left(1 - 0.114 \frac{T_t}{W}\right) = - 0.000468$$

$$e = 0$$

Since the coefficient e is equal to zero the characteristic Equation (VI-16) is reduced to a cubic equation and Routh's discriminant is (29)

$$R = bc - ad \qquad \text{(VI-27)}$$

which is calculated to be 0.001038. This value is significant only in that it is greater than zero, and the motion is stable.

To better define the motion of the helicopter it is convenient to determine from the characteristic equation the period of the oscillations and the time required for the oscillations to halve in amplitude. The coefficients found above placed in Equation (VI-16) give the cubic equation

$$0.0037 \lambda^3 + 0.2373 \lambda^2 + 0.00437 \lambda + 0.000468 = 0 \qquad \text{(VI-28)}$$

The roots of this equation are found to be:

$$\lambda_1 = - 64.07$$

$$\lambda_{2,3} = - 0.0141 \pm 0.0545i$$

The first root is a non-oscillatory, highly damped mode, and the other roots define the lightly damped phugoidal mode. The period of the phugoid is (30)

$$P = \frac{2\pi}{0.0545} = 115 \text{ seconds}$$

and the time to damp to half amplitude is equal to

$$\frac{0.693}{0.0141} = 49.2 \text{ seconds}$$

The approximation of the period of oscillation suggested by Gessow and Myers (31) will be used as a basis of comparison. This equation in the notation of this report is given by (32)

$$P = \frac{2\pi}{\sqrt{g}} \left[\frac{-\frac{da'}{da_1} \frac{\partial a_{1_s}}{\partial q}}{\frac{\partial a_{1_s}}{\partial V}} \right]^{1/2} \qquad \text{(VI-29)}$$

Substituting in the appropriate values of the derivatives gives a period of 150.2 seconds. Though this approximation differs considerably from the period found above, it does substantiate the fact that a long period phugoid does exist. This is a desirable characteristic of the helicopter motion in that the pilot will easily be able to react with controls to eliminate the oscillations due to disturbances from hovering equilibrium.

CHAPTER VII

DISCUSSION OF RESULTS

The proposed design is penalized by having an increased vertical drag due to the wing and a loss of power available due to that used by the tail shrouded propeller in hovering. However, in Figure 17, Appendix IX, it is seen that this vertical drag handicap in hovering is offset by the reduction of the power required during the lower flight range when the wings unload the rotors. The thrust of the tail shroud is used to advantage at low forward velocity, but this power loss, resulting from use of the shroud as a control force in hovering flight, is justified to a greater extent in the simplified rotor head and control system of the helicopter.

This rapid drop in the power required when going from the static condition to forward flight will also be of advantage when operating at high density altitudes or when operating over gross weight. For example, in Figure 16, Appendix IX, it is seen that the power required for flight is reduced 26.8 per cent with a ground run up to a velocity of 20 feet per second (approximately 14 miles per hour).

From Table 8, Appendix IX, it can be seen that the coning angle is extremely small on the single-bladed rotor. This reduced coning angle will first reduce the periodic air force caused by the different inflow angles of the coned rotor in forward flight, thus reducing vibrations (33). The rotor itself is more stable with the reduced coning angle because the blade mass is distributed more in the plane of rotation. This

tends to eliminate the problem of blade weaving (34). In general, it can be concluded that all the problems associated with asymmetric blade loadings will be reduced by the small coning angle.

In the stability analysis it is shown that the helicopter is stable and has a long period of oscillation. Since the motion is very slow the pilot will be able to readily correct for this phugoidal mode, and even an unstable oscillation could be tolerated. The long period oscillations of the proposed design are the result of several things. The most important of which are: first, since the blade has a very low coefficient of thrust the blade flapping with forward velocity is very small, and next, the very high effective mass number increases damping.

CHAPTER VIII

CONCLUSIONS

The proposed design appears to be a feasible approach to a small, easy to construct helicopter that has good stability and control characteristics.

The use of the shrouded tail propeller offers adequate control in hover, and the power utilized is not a loss at forward velocities. The tail shroud as a control in hover eliminated the need of cyclic pitch input to the rotors, thus simplifying construction and reducing costs. Though not covered in this report, it is obvious that the stability in forward flight will be greatly increased by the tail shroud (35).

The disadvantages of the weight and vertical drag in hover of the stub wings are somewhat offset by the unloading of the main rotors in forward flight. However, the wings are primarily a fairing for the lateral rotor supports and drive; the disadvantages pertaining to the wings have to be further weighed against the merits of the configuration as a whole.

As previously mentioned, the configuration is an attempt to provide a helicopter that is stable and easy to fly. The lateral stability will be increased considerably over the conventional helicopter, because of the increased moment of inertia in roll resulting from the wing and lateral rotors. It has been shown that the longitudinal hovering stability is very satisfactory, realizing that it is even common to have a diverging phugoidal mode at a much shorter period of oscillation. Thus,

the overall increased stability will help eliminate some of the pilot-induced oscillations resulting from the over-controlling of a sensitive machine.

Having thus determined that the helicopter is stable and has adequate control about all axes, the performance must be such that the rotorcraft will be acceptable. The machine was designed to have an endurance of 2 hours, with a 30-minute fuel reserve at cruising speed. Using slightly over 50 per cent of the power available, a cruise of 70 knots can be obtained. This is satisfactory, and this cruise capability should make the machine attractive in the private plane field. Though the hovering ceiling out of ground effect is not too high, the machine is capable of operating from high terrain when ground effect is considered or when a running take-off is utilized.

APPENDICES

APPENDIX I

HELICOPTER DIMENSIONS AND CONFIGURATION

Table 1. Helicopter Dimensions

Item	Size
1. Main Rotor:	
Blade radius	9.50 ft.
Counter-weight radius	4.75 ft.
Blade chord	8.35 in.
Rotor height above ground	5.56 ft.
2. Tail Shroud and Propeller:	
Shroud diameter (inlet)	3.00 ft.
Shroud chord (length)	2.00 ft.
Propeller diameter	3.00 ft.
Propeller chord	4.24 in.
3. Wing:	
Span	14.50 ft.
Chord	30.00 in.
Maximum thickness	6.30 in.
4. Fuselage:	
Length (including shroud)	14.93 ft.
Width	2.27 ft.
Height	3.69 ft.

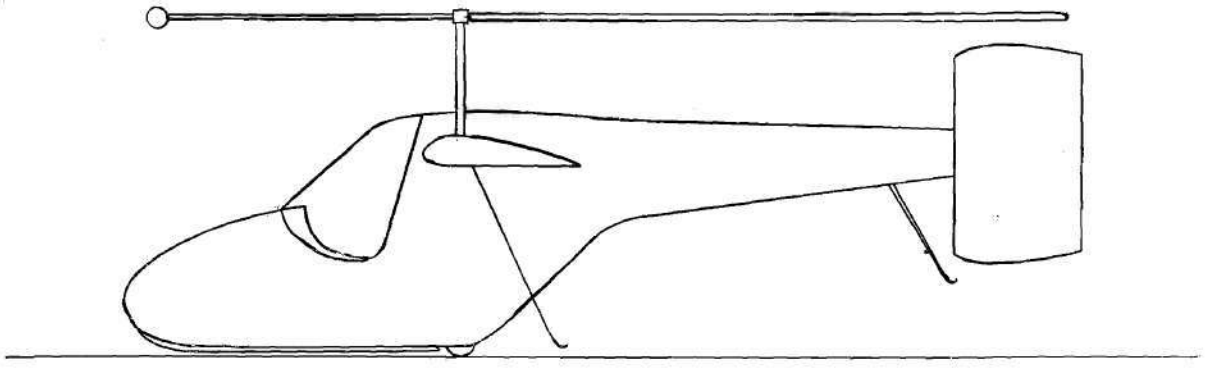

Figure 6. Side View of Helicopter

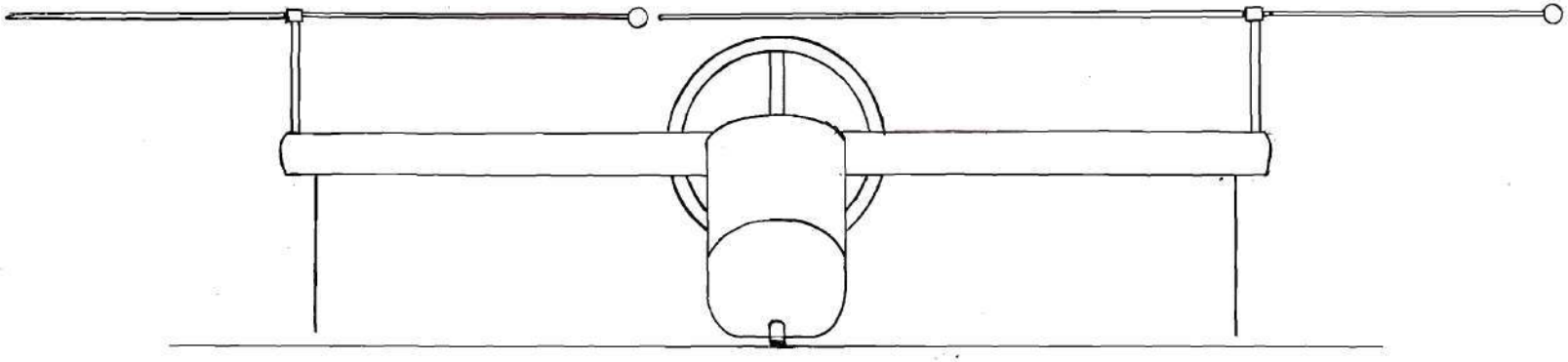

Figure 7. Front View of Helicopter

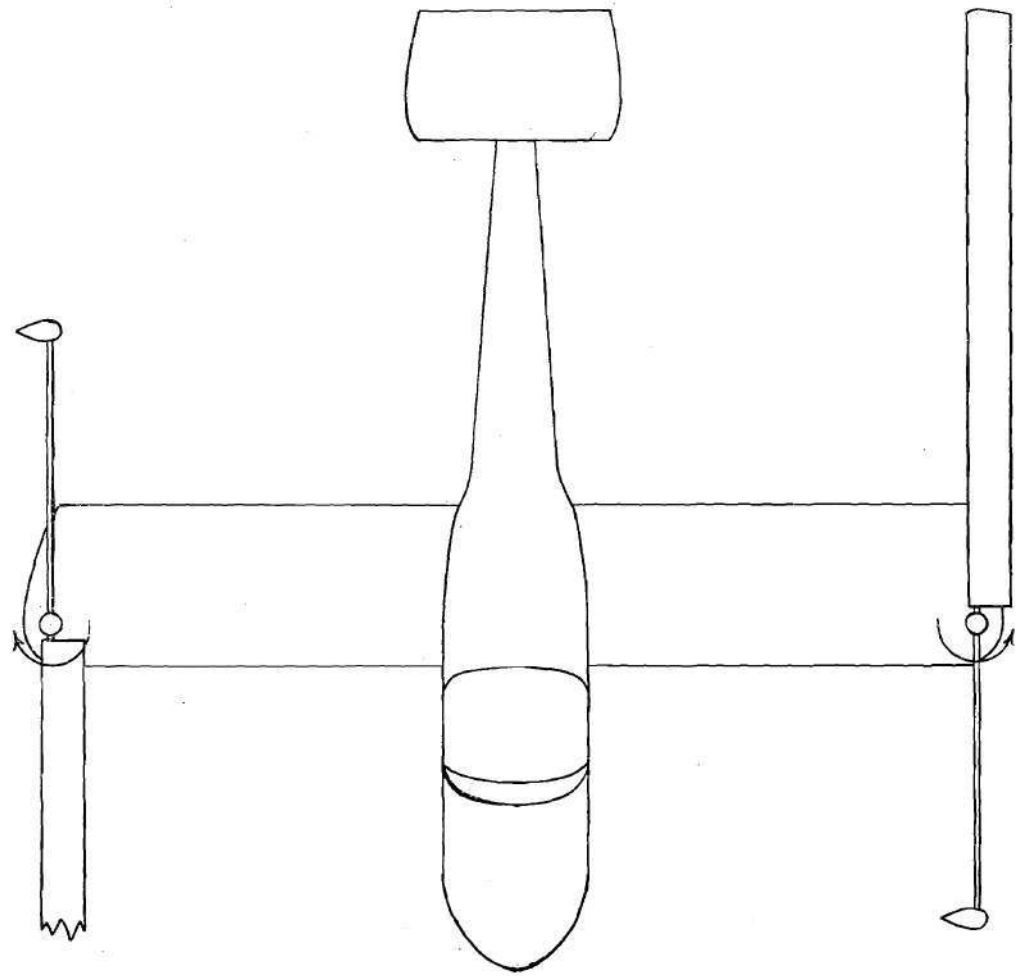

Figure 8. Top View of Helicopter

APPENDIX II

WEIGHT AND BALANCE DETERMINATION

For the weight and balance data the longitudinal reference station is at the rotor mast (see Figure 9). In the Tables the stations are in inches from this station and are positive forward and negative aft. The ground plane is used as the vertical reference line. The components are so placed that the center of gravity at gross weight is on the horizontal reference line. Weight estimates are based on the construction, as discussed in Chapter IV and as given for the main rotor in Appendix III.

With the fuel exhausted (the only expendable load) the center of gravity travel can be computed from the table of weights and moments, as follows:

$$\begin{array}{r} -4460 \text{ in. lbs.} \\ 4280 \text{ in. lbs.} \\ \hline -180 \text{ in. lbs. moment unbalance} \end{array}$$

$$\text{center of gravity travel} = \frac{-180}{850 - 72} = -0.232 \text{ in.}$$

Hence the center of gravity travel will be less than one-quarter inch. This can easily be compensated for with the tail thrust.

The estimated centers of gravity of Figure 9 are numbered as they are in Table 2.

Table 2. Weight and Balance

	Item	Weight lbs.	Horizontal Station in.	Horizontal Moment in. lbs.	Vertical Station in.	Vertical Moment in. lbs.
1.	Pilot	190	21.5	4080	17.5	3325
2.	Fuel	72	2.5	180	43.0	3100
3.	Fuselage and Controls	200	1.0	200	18.5	3700
4.	Wing	80	- 4.5	- 360	39.5	3160
5.	Engine	79	0.0	0	21.0	1660
6.	Tail Propeller and Shroud	41	- 100.0	- 4100	38.0	1560
7.	Rotor Drive and Gear Boxes	50	0.0	0	39.5	1975
8.	Main Rotors	88	0.0	0	66.7	5870
9.	Design Pick-up	50	0.0	0	0.0	0

Gross Weight	850 lbs.
Horizontal c.g.	0.0 in.
Vertical c.g.	28.6 in.

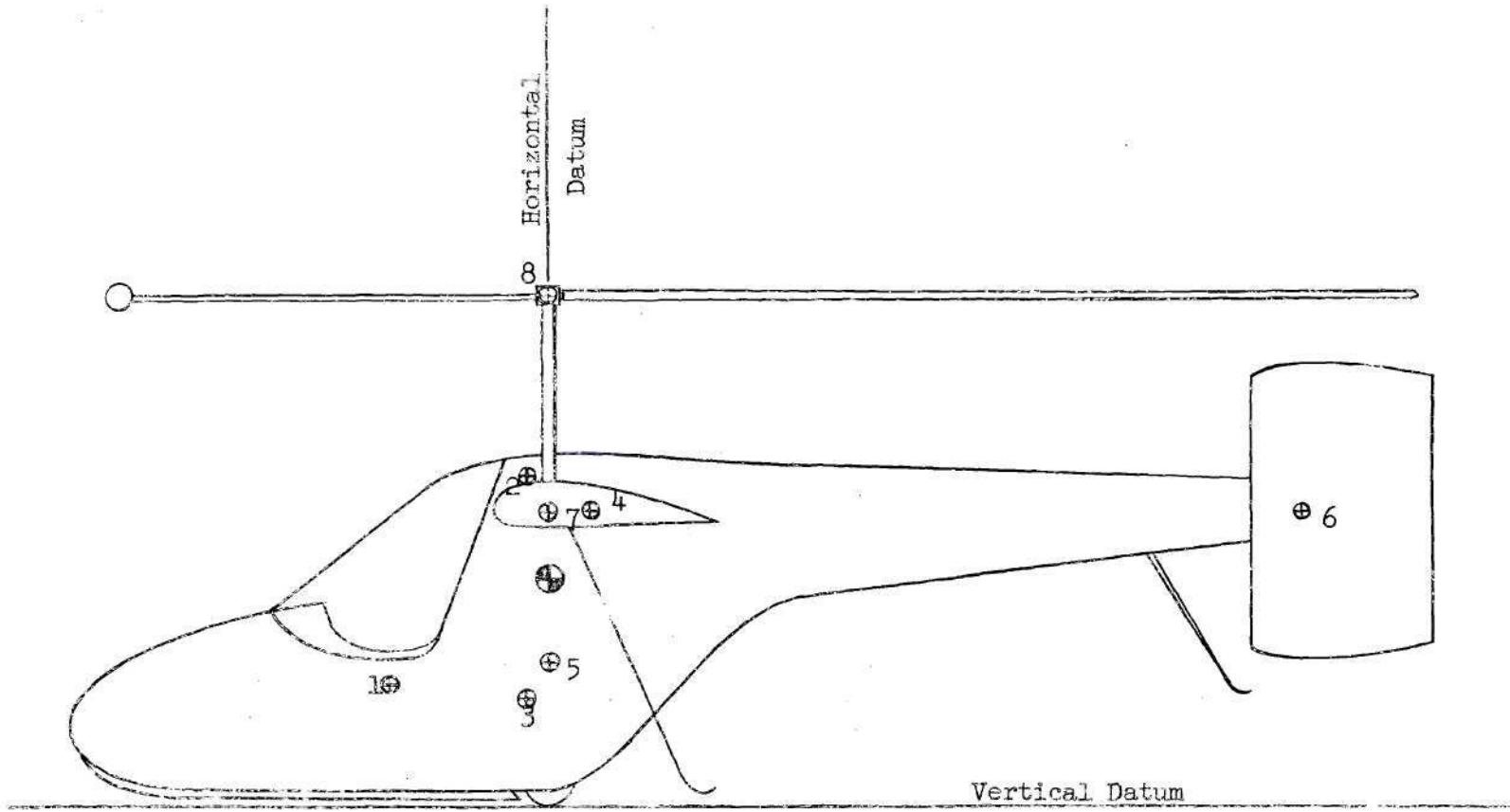

Figure 9. Helicopter Balance Diagram

APPENDIX III

DETAILS OF MAIN ROTOR BLADE

The following detailed construction analysis will give a blade that will be easy to fabricate, require little maintenance, and be sufficiently rigid, considering the very low disc loading to avoid coupled bending and torsion.

Summarizing the blade characteristic shape:

Airfoil	NACA 0015
Blade radius	9.50 ft.
Counter-weight radius	4.75 ft.
Spar tube length	14.25 ft.
Spar tube diameter	1.00 in.
Blade chord	8.35 in.
Blade maximum thickness	1.252 in.

The blade construction will be as shown in Figure 10, with the ribs spaced six inches apart. The structure will be covered with 3/64 inch three-ply birch plywood and finished with aircraft fabric and dope. The steel tube spar is centered at the aerodynamic center (quarter chord) of the blade, and the blade is balanced with an Everdur 1015 bar noseweight, such that the quarter chord will also be the chordwise center of gravity. In Table 3 the component weights were computed and then the size of the noseweight was determined to properly balance the blade. The weight estimates were based on aircraft material weights as given by K. D. Wood. The rotor blade component weights and stations were estimated from the blade cross-section appearing in Figure 11. The running weight

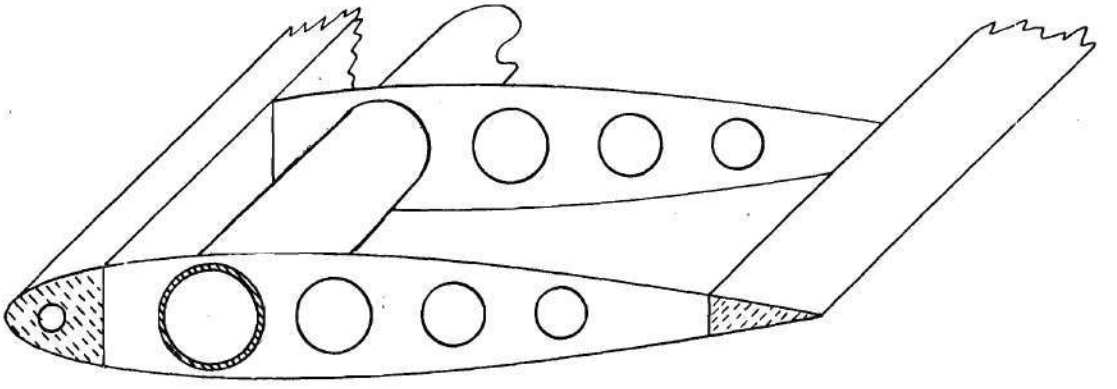

Figure 10. Rotor Blade Structure

of the main rotor was thus calculated to be 1.776 pounds per foot of blade span.

The size of the counter-weight was determined using this blade structural weight as a basis. The total weight of the balanced blade was determined from the weight distribution shown in Figure 12. From this figure the total weight of the rotor is seen to be 35.25 pounds.

The moment of inertia of the blade about its hinge line can be calculated from the known data by considering the three concentrated weights of the blade, the counter-weight arm, and the counter-weight. The moment of inertia of the rotor is calculated as follows (36):

$$I_{blade} = \frac{MR^2}{3} = \frac{W_b R^2}{3g} = \frac{(16.87)(9.5)^2}{(3)(32.2)} = 157.10 \text{ slug-feet}^2$$

$$I_{spar} = \frac{W_S R_S^2}{3\,g} = \frac{(3.08)(4.75)^2}{(3)(32.2)} = 0.72$$

$$I_{C.W.} = \frac{W_{c.w.} R_{c.w.}^2}{g} = \frac{(15.3)(4.75)^2}{32.2} = 10.72$$

Moment of inertia of rotor $168.54 \text{ slug-feet}^2$

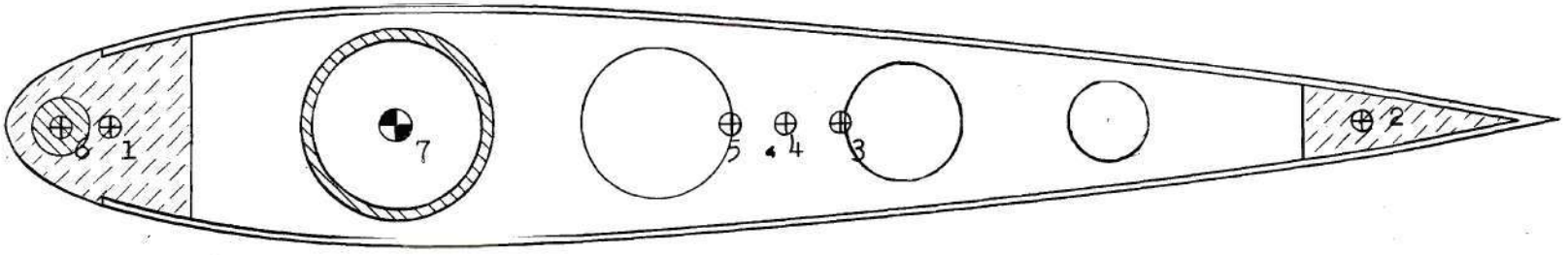

Figure 11. Main Rotor Construction

Table 3. Blade Structural Data

	Component (material)	Weight/foot pounds	Station inches
1.	Leading edge (sweet birch)	0.294	1.50
2.	Trailing edge (Sitka spruce)	0.0466	- 5.24
3.	Skin (3/64 inch, 3-ply birch)	0.276	- 2.40
4.	Doped fabric (aircraft linen)	0.994	- 2.10
5.	Ribs at two per foot (1/16 inch, 3-ply birch)	0.0177	- 1.80
6.	Noseweight (Everdur 1015)	0.393	1.80
7.	Spar tube (stainless steel)	0.6491	0.00

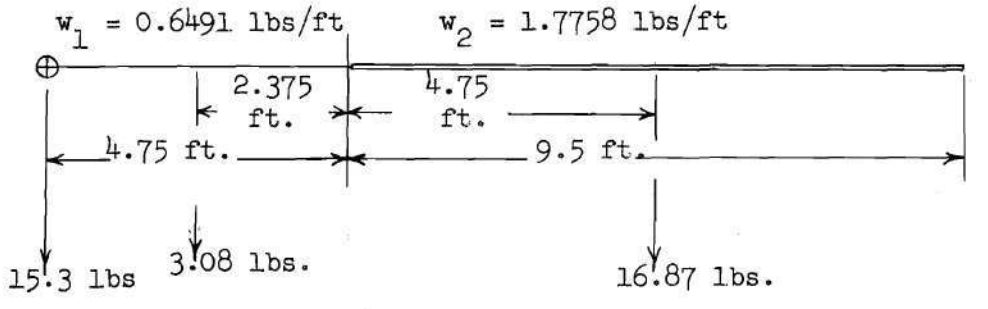

Figure 12. Weight and Balance of Main Rotor

Figure 13. Rotor Weights in Determining Moment of Inertia

APPENDIX IV

ESTIMATION OF MOMENT OF INERTIA OF HELICOPTER IN PITCH AND YAW

In the calculation of the moments of inertia of the components about their own center of gravity, the bodies were broken up into standard shapes for closer approximations. The tabulated data appears in Tables 4 and 5 for the computation of the helicopter moments of inertia.

Table 4. Moment of Inertia in Pitch

	Item	Weight pounds	J_o pounds-inch^2	r inch	Wr^2 pounds-inch^2
1.	Pilot	190	1,200	24.0	109,300
2.	Fuel	72	0	14.5	15,140
3.	Fuselage and Controls	200	36,658	10.3	21,200
4.	Wing	80	202,000	11.8	11,130
5.	Engine	79	4,000	7.6	4,560
6.	Tail Propeller and Shroud	41	0	100.0	400,000
7.	Rotor Drive and Gear Boxes	50	0	10.8	5,830
8.	Main Rotors	88	0	38.1	127,800
9.	Design Pick-up	50	0	0.0	0

$$J_y = \sum J_o + \sum Wr^2 = 938,818 \text{ lbs.-in.}^2$$

$$I_y = 202 \text{ slug-feet}^2$$

Table 5. Moment of Inertia in Yaw

	Item	Weight pounds	J_o pounds-inch^2	r inch	Wr^2 pounds-inch^2
1.	Pilot	190	1,140	21.5	87,800
2.	Fuel	72	0	2.5	450
3.	Fuselage and Controls	200	36,658	1.0	200
4.	Wing	80	205,000	- 4.5	1,640
5.	Engine	79	3,290	0.0	0
6.	Tail Propeller and Shroud	41	0	- 100.0	410,000
7.	Rotor Drive and Gear Boxes	50	0	87.0	378,500
8.	Main Rotors	88	782,000	87.0	666,000
9.	Design Pick-up	50	0	0.0	0

$$J_z = \sum J_o + \sum Wr^2 = 2,572,178 \text{ lbs.-in.}^2$$

$$I_z = 555 \text{ slug-feet}^2$$

APPENDIX V

ESTIMATION OF VERTICAL DRAG

In Chapter V the assumptions are outlined which govern the computation of the vertical drag in hovering flight. These assumptions are summarized for convenience:

1. Fully contracted downwash.
2. Wing flap lowered 60 degrees.
3. Bodies in downwash drag have a coefficient of drag of 1.0.
4. Surface area in downwash is approximated by wing area with 50 per cent chord flap lowered.

The downwash velocity in the fully developed wake is twice the induced velocity at the rotor disc.

$$v_i = \sqrt{\frac{\Delta p}{2\rho}} = \sqrt{\frac{1.5}{(2)(0.002378)}} = 17.8 \text{ ft./sec.}$$

$$V_v = 2v_i = 35.6 \text{ ft./sec.}$$

The dynamic pressure in the hovering rotor wake is

$$q_v = \frac{1}{2} \rho V_v^2 = \frac{1}{2}(0.002378)(35.6)^2 = 1.51 \text{ lbs./ft.}^2$$

The rotor downwash area is one-half the rotor area, and hence the rotor wake radius is

$$R_w = \frac{9.5}{\sqrt{2}} = 6.7 \text{ ft.}$$

Thus the area in the downwash will be approximated by the projected wing area with the flap lowered 60 degrees. This area is found to be 27.2 square feet and the vertical drag is

$$D_v = C_D \, q \, S = (1.0)(1.51)(27.2) = 41.0 \text{ lbs.}$$

This will give an increase in thrust required of 20.5 pounds per rotor in hovering flight. From

$$\frac{891 - 850}{850} \times 100\% = 4.81\%$$

it is seen that this constitutes less than a 5 per cent increase in hovering thrust required.

APPENDIX VI

CALCULATION OF POWER REQUIRED IN HOVERING FLIGHT

In the determination of the power required in hovering flight, the performance parameters and techniques will be used as presented by Stevens. Since this thesis applies to single rotor helicopters, the analysis will be modified for the proposed design of this paper as discussed in Chapter V.

The power required is calculated as follows:

gross weight	850 lbs.
vertical drag	41 lbs.
thrust in hover	891 lbs.

The thrust is approximately equal to the weight plus vertical drag

$$C_T = \frac{W/2}{\rho \pi \Omega^2 R^4} = \frac{891/2}{(0.002378)(3.14)(63.2)^2(9.5)^4}$$

$$C_T = 0.00184$$

The coefficient of torque is equal to

$$C_Q = C_{Q_L} + \Delta C_{Q_{DP_c}} + \Delta C_{Q_{DP_v}} + \Delta C_{Q_{a_o}} + \Delta C_{Q_s} + \Delta C_{Q_t}$$

$$\Delta C_{Q_L}: \quad \frac{\Delta C_{Q_L}}{C_T} = 0.031$$

$$\Delta C_{Q_L} = (0.031)(0.00184) = 0.000057$$

adding 20 per cent for the single blade

$$1.2\ \Delta C_{Q_L} = 0.0000684$$

$\Delta C_{Q_{DP_c}}$:

$$\frac{\Delta C_{Q_{DP_c}}}{\delta_o \sigma} = 0.1251$$

$$\Delta C_{Q_{DP_c}} = (0.1251)(0.008)(0.0233) = 0.0000233$$

$\Delta C_{Q_{DP_v}}$:

$$\frac{\Delta C_{Q_{DP_v}}}{\epsilon \bar{C}_L C_T} = 0.75$$

$$\alpha = \frac{\bar{C}_L}{a} = \frac{0.45}{6.28} = 0.0717$$

$$\Delta C_{Q_{DP_v}} = (0.75)(0.008)(0.45)(0.00184) = 0.00000497$$

$\Delta C_{Q_{a_o}}$:

$$\Delta C_{Q_{a_o}} = \frac{a_o{}^2 \mu^2 \sigma a}{72} (\epsilon a - 1) = 0$$

($\mu = 0$ in hover)

ΔC_{Q_s} : In the hovering case with $\bar{C}_L = 0.45$ tip stall is not a factor.

ΔC_{Q_t} : The blade tip loss is negligible.

Therefore,

$$C_Q = C_{Q_L} + C_{Q_{DP_c}} + C_{Q_{DP_v}} = 0.00009667$$

and

$$Q = C_Q \rho \pi \Omega^2 R^5$$

$$= (0.00009667)(0.002378)(3.14)(63.2)^2(9.5)^5$$

$$Q = 222.5$$

The torque due to the rotor counter-weight is

$$Q_{C.W.} = (D_{C.W.})(r) = (0.322)(4.75) = 1.53$$

thus,

$$Q_{total} = Q + Q_{C.W.} = 222.5 + 1.53 = 224.03$$

The horsepower required for each rotor is

$$HP = \frac{\Omega Q}{550} = \frac{(63.2)(224.03)}{550} = 25.8$$

Adding the horsepower required for the tail propeller and considering both rotors,

$$HP = 2(25.8) + 3.5 = 55.1$$

and adding 5 per cent for rotor drive losses gives

$$HP_{req.} = 55.1 + 2.8 = 57.9$$

The excess power available in hover is therefore

$$\frac{64.8 - 57.9}{57.9} \times 100\% = 11.93\%$$

APPENDIX VII

CALCULATION OF HOVERING CEILING

The power available from the 72 horsepower engine will be reduced by 10 per cent for cooling losses, giving the power available for the rotor drive to be 64.8 horsepower. The power available at altitude will vary as the air density (see Table 6).

The horsepower required will be calculated as shown in Appendix VI. The coefficient of thrust is seen to vary inversely as the air density, and the torque of the counter-weight varies directly as the density. The parameters which determine the power required for various altitudes are given in Table 7.

The horsepower available and required versus altitude are shown in Figure 14. From this it is seen that the hovering ceiling is approximately 3,200 feet. When ground effect with its 20 per cent reduction in power required is calculated versus altitude, it is seen that the hovering ceiling in ground effect is over 8,000 feet.

Table 6. Horsepower Available Versus Altitude

Altitude	Density	σ	$HP_{available}$
0	0.002378	1.0000	64.8
2,000	0.002242	0.9427	61.0
4,000	0.002112	0.8880	57.5
6,000	0.001988	0.8358	54.1
8,000	0.001859	0.7859	50.1
10,000	0.001755	0.7385	47.8

Table 7. Horsepower Required Versus Altitude

	Altitude		
	2,000	4,000	6,000
C_T	0.001945	0.002065	0.002195
$\frac{\Delta C_{Q_L}}{C_T}$	0.0325	0.0340	0.350
$\frac{\Delta C_{Q_{DP_c}}}{\delta_o \sigma}$	0.125111	0.12512	0.125125
$\frac{\Delta C_{Q_{DP_v}}}{\bar{C}_L C_T}$	0.75	0.75	0.75
$1.2\Delta C_{Q_L}$	0.0000759	0.0000843	0.0000922
$\Delta C_{Q_{DP_c}}$	0.0000233	0.0000233	0.0000233
$\Delta C_{Q_{DP_v}}$	0.00000525	0.00000558	0.00000592
C_Q	0.00010445	0.00011318	0.0001242
Q	227.0	231.0	233.5
$Q_{C.W.}$	1.44	1.36	1.28
Q/rotor	228.44	232.36	234.78
HP/rotor	26.3	26.7	27.0
HP_{total}	56.1	56.9	57.6
$HP_{required}$	58.9	59.7	60.4
$HP_{required\ in\ ground\ effect}$	47.1	47.8	48.3

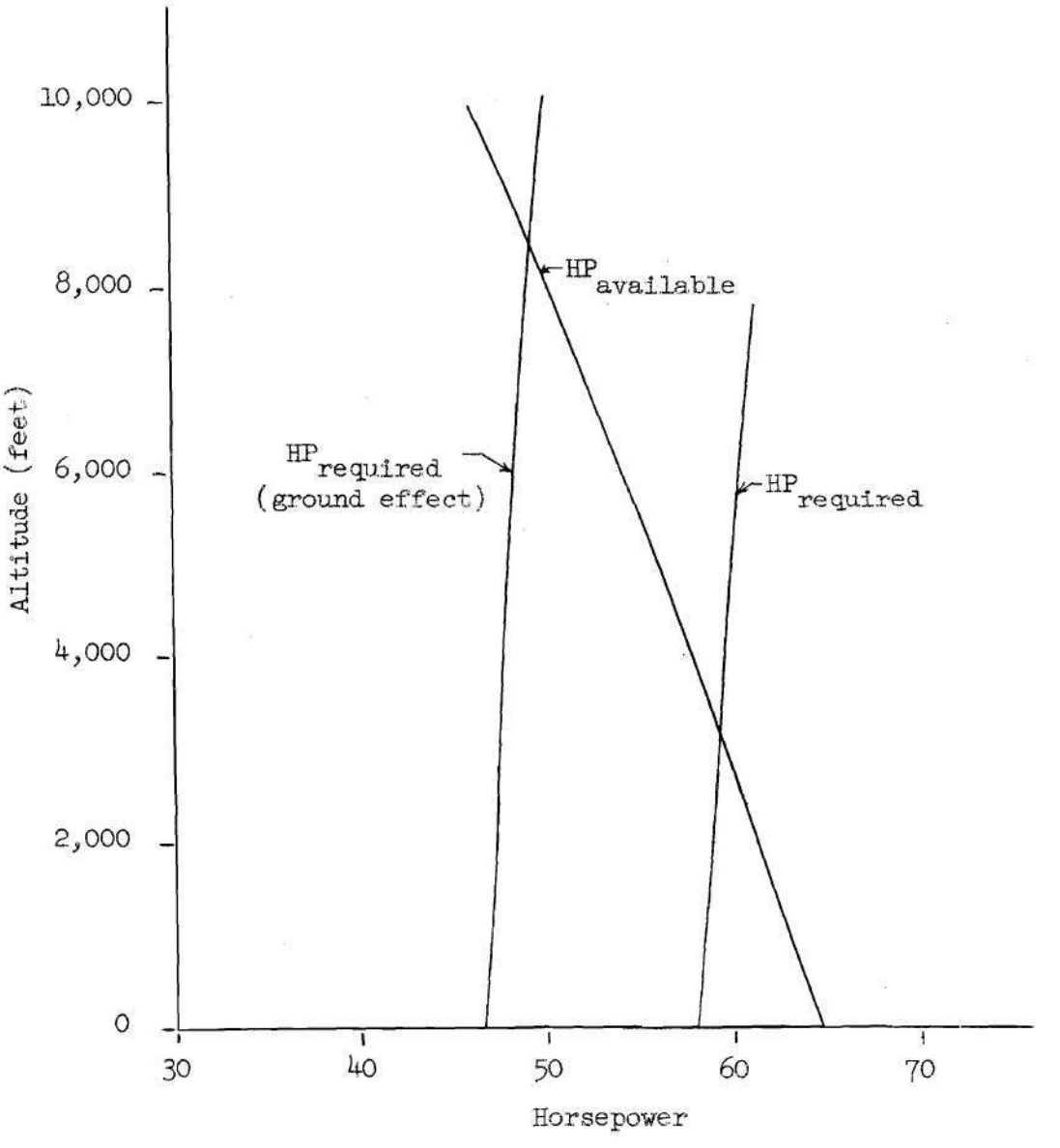

Figure 14. Horsepower Required Versus Altitude

APPENDIX VIII

ESTIMATION OF DRAG IN FORWARD FLIGHT

The drag area as defined by Hoerner will be used to define the drag of the various components of the helicopter (37). Hoerner will be used as the reference in this section and will not be cited further.

The drag area of the components are estimated as follows:

Fuselage

$S_w = 88.0 \text{ ft.}^2$

$C_f = 0.005$

$D_f = C_f q S_w$

$f = \frac{D_f}{q} = C_f S_w = (0.005)(88.0) = 0.44 \text{ ft.}^2$

Wing

$A = 5.8$

$c = 2.5 \text{ ft.}$

$S = 36.3 \text{ ft.}^2$

$S_{exposed} = 30.67 \text{ ft.}^2$

$t/c = 0.21$

$C_f = 0.0028$

thickness correction

$C_{D_s}/2C_f = 1 + 2t/c + 100(t/c)^4 = 1.62$

$f = (1.62)(2)(0.0028)(30.67) = 0.278 \text{ ft.}^2$

Rotor Masts

Area = (2 in. x 24 in.)/mast

$S = 96 \text{ in.}^2$

$C_D = 1.0$

$f = (1.0)(96/144) = 0.667 \text{ ft.}^2$

Rotor Hubs

Area = (5 in. x 2.5 in.)/hub

$S = 25 \text{ in.}^2$

$C_D = 0.35$

$f = (0.35)(25/144) = 0.0607 \text{ ft.}^2$

Wheel

$S = 24 \text{ in.}^2$

$C_D = 0.18$

$f = (0.18)(24/144) = 0.03 \text{ ft.}^2$

Outrigger Struts

Area = (40 in. x 1.0 in.)/strut

$S = 80 \text{ in.}^2$

$C_D = 0.9$

$f = (0.9)(80/144) = 0.5 \text{ ft.}^2$

Interference Drag (Wing)

$C_{D_t} = \Delta D/qt^2$

$f = (2)C_{D_t} t^2 = (2)(0.16)(0.04) = 0.0128 \text{ ft.}^2$

The total parasite drag area is found to be 1.989 square feet. Ten per cent is added to this to account for the strut and rotor mast

interference drag and to insure a conservative estimate, making the drag area 2.187 square feet.

The induced drag area of the wing is computed based on a coefficient of lift of 0.4. Taking into consideration the tip losses, the induced drag area is found to be 0.287 square feet.

APPENDIX IX

DETERMINATION OF HORSEPOWER REQUIRED FOR FORWARD SPEED

In the calculation of the thrust required for forward velocity, the composite drag term, D_f , must be determined for the range of forward velocities anticipated. In Figure 15 it will be noted that the thrust of the tail shrouded propeller by the definition of drag will be negative in the lower velocity range. The drag term, D , is the sum of the parasite and induced drag of the helicopter, and the composite drag, D_f , is the sum of the drag and thrust mentioned. The induced drag is assumed to be the same percentage of the total drag that it is in cruise flight. This simplification is made to eliminate the necessity of computing the composite drag for the various angles of attack of the wing in the iterative process of determining the helicopter pitch angle, Θ_y .

The method of determining the horsepower required will be illustrated for a representative forward velocity of 40 feet per second. From Figure 15 the composite drag for this velocity is found to be - 32 pounds. As a first approximation using Equation (V-2)

$$\tan \Theta_y = - \frac{D_f \cos \phi_c}{W - D_f \sin \phi_c} = - \frac{(-32)(1.0)}{850} = 0.0376$$

$$\Theta_y = 2.16^\circ$$

$$\alpha_w = 5.93^\circ + 2.16^\circ = 8.09^\circ$$

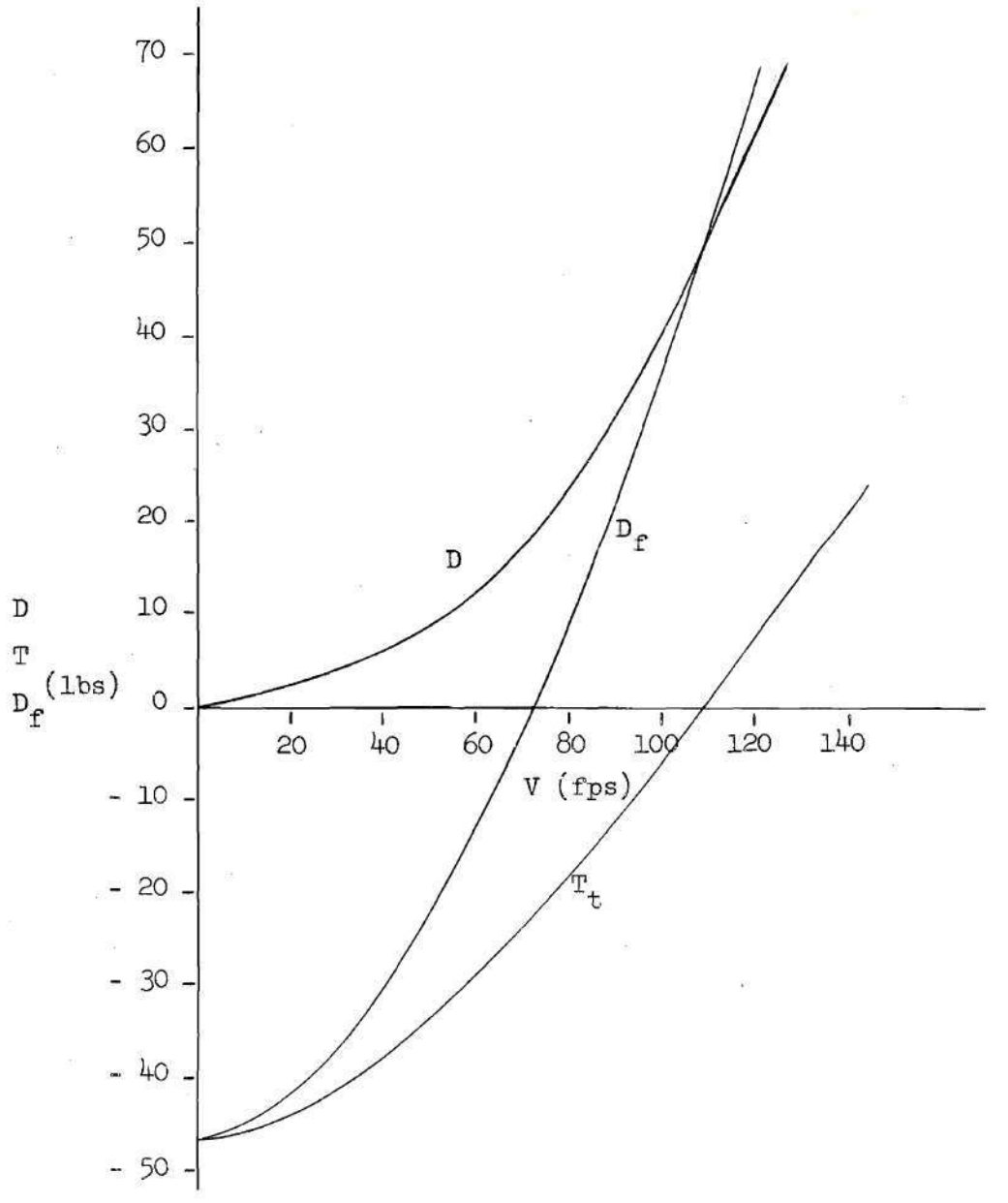

Figure 15. Composite Drag Versus Velocity

for this angle of attack

$$C_L = 0.90$$

$$L = C_L\, 0.5\rho\, V^2 S = (0.90)(0.5)(0.002378)(40)^2(36.3)$$

$$L = 62.2 \text{ lbs.}$$

$$T = W - L = 850 - 62.2 = 787.8 \text{ lbs.}$$

Using this weight for a second approximation of θ_y in Equation (V-2) gives

$$\tan \theta_{y_2} = - \frac{(-32)(1.0)}{787.8} = 0.0406$$

$$\theta_{y_2} = 2.33°$$

$$\alpha_{w_2} = 5.93° + 2.33° = 8.26°$$

$$C_{L_2} = 0.92$$

$$L_2 = (0.92)(0.5)(0.002378)(40)^2(36.3) = 63.6 \text{ lbs.}$$

$$T_2 = W - L_2 = 850 - 63.6 = 786.4 \text{ lbs.}$$

Repeating this process for a third approximation of θ_y,

$$\tan \theta_{y_3} = - \frac{(-32)(1.0)}{786.4} = 0.0407$$

$$\theta_{y_3} = 2.33°$$

$$\alpha_{w_3} = 5.93° + 2.33° = 8.26°$$

The pitch angle having thus converged leads to the parameters required for determining the rotor X-force which are:

$$v_a = \frac{V \sin \alpha_r}{\Omega R} = \frac{(40)(0.0407)}{(63.2)\ (9.5)} = 0.00271$$

where

$$\alpha_r = \theta_y + \phi_c = 2.33° + 0.0 = 2.33°$$

and

$$\mu = \frac{V \cos \alpha_r}{\Omega R} = \frac{(40)(0.992)}{(63.2)(9.5)} = 0.0667$$

For a first approximation of the coefficient of thrust found by Equation (V-7) use Equation (III-1)

$$C_{T_1} = \frac{W/2}{\rho \pi \Omega^2 R^4} = \frac{786.4/2}{(0.002378)(3.14)(63.2)^2(9.5)^4}$$

$$C_{T_1} = 0.001625$$

Using the work by Stevens as a guide the rotor X-force is found from

$$F_X = \frac{1}{2} C_X \rho \pi \Omega^2 R^4$$

where

$$C_X = \Delta C_{X_L} + \Delta C_{X_{DP_c}} + \Delta C_{X_{DP_v}}$$

It is assumed here, as previously stated, that the tip losses are negligible and that retreating blade stall is not a factor. From appropriate figures in the reference

$$\frac{\Delta C_{X_L}}{C_T} = -0.003$$

$$\Delta C_{X_L} = (-0.003)(0.001625) = -0.00000488$$

$$\frac{\Delta C_{X_{DP_c}}}{\delta_o \sigma} = 0.02502$$

$$\Delta C_{X_{DP_c}} = (0.02502)(0.008)(0.0233) = 0.00000466$$

and

$$\Delta C_{X_{DP_v}} = -\frac{16\epsilon}{\sigma}\left(\frac{C_T}{1-u^2}\right)^2 u$$

$$= -\frac{(16)(0.008)}{0.0233}\left(\frac{0.001625}{1-0.0677^2}\right)^2 0.0677$$

$$\Delta C_{X_{DP_v}} = -0.00000974$$

Summing these components gives

$$C_X = -0.000001194$$

and

$$F_X = - 0.145$$

The drag of the counter-weight on the rotor will alter this to give a final X-force of 0.177. The pitch attitude angle can now be refined, taking into account this X-force and using Equation (V-1) to give

$$\tan \Theta_{y_4} = - \frac{D_f \cos \phi_c + F_X \cos \Theta_y}{W - D_f \sin \phi_c + F_X \sin \Theta_y}$$

$$\tan \Theta_{y_4} = - \frac{- 16 + (0.177)(0.992)}{393.2 + (0.177)(0.0407)} = 0.0402$$

$$\Theta_{y_4} = 2.31°$$

$$\alpha_{w_4} = 5.93° + 2.31° = 8.24°$$

$$C_{L_4} = 0.91$$

$$L_4 = (0.91)(0.5)(0.002378)(40)^2(36.3) = 63.0 \text{ lbs.}$$

$$T_4 = 850 - 63 = 787 \text{ lbs.}$$

and from Equation (V-7)

$$C_{T_4} = \frac{393.5 + (0.177)(0.0403)}{(0.002378)(3.14)(63.2)^2(9.5)^4(0.9992)}$$

$$C_{T_4} = 0.00163$$

This coefficient of thrust differs from the first approximation by such a small amount that the X-force will not vary and further iteration will not be necessary. The torque will next be determined using the process as outlined in Appendix VI. The coefficient of torque is found from

$$C_Q = \Delta C_{Q_L} + \Delta C_{Q_{DP_c}} + \Delta C_{Q_{DP_v}}$$

where

$$\frac{\Delta C_{Q_L}}{C_T} = 0.008$$

$$1.2 \quad C_{Q_L} = (1.2)(0.008)(0.00163) = 0.00001565$$

$$\frac{\Delta C_{Q_{DP_c}}}{\delta \sigma} = 0.1253$$

$$\Delta C_{Q_{DP_c}} = (0.1253)(0.008)(0.0233) = 0.0000234$$

$$\frac{\Delta C_{Q_{DP_v}}}{\epsilon \overline{C}_L C_T} = 0.74$$

where

$$\overline{\alpha} = \frac{6C_T}{a \sigma} = 0.0669$$

$$\overline{C}_L = \frac{6C_T}{\sigma} = 0.42$$

thus

$$\Delta C_{Q_{DP_v}} = (0.74)(0.008)(0.42)(0.00163) = 0.00000405$$

Summing these components gives

$$C_Q = 0.0000431$$

$$Q = (0.0000431)(0.002378)(3.14)(63.2)^2(9.5)^5 = 99.5$$

Adding the torque due to the drag of the rotor counter-weight gives the total torque required per rotor to be 101.03 foot-pounds. The horsepower required per rotor is

$$HP = \frac{\Omega Q}{550} = \frac{(63.2)(101.03)}{550} = 11.6$$

The total horsepower required will be the power required for the two rotors, the power required for the tail shrouded propeller, plus a 5 per cent power loss in the rotor drive. This gives

$$HP_{required} = 1.05 \left[2(11.6) + 2.83 \right] = 27.33$$

as the total horsepower required of the helicopter to fly at a forward velocity of 40 feet per second. Table 8 gives the various parameters computed for velocities throughout the operating range. The horsepower required versus forward velocity is given in Figure 16. It is seen from this figure that the best endurance will be at 80 feet per second and the best range at a velocity of 100 feet per second (38).

A comparison of the proposed design will be made with a Bristol

type 171, Mk. 3, (39). The total horsepower required will be converted to a coefficient of torque by the equations

$$Q = \frac{HP\ 550}{\Omega}$$

$$C_Q = \frac{Q}{\rho\ \pi\ \Omega^2 R^5}$$

This equivalent torque coefficient for several advance ratios is found, and the ratio is taken for sake of comparison with the static coefficient of torque. The advance ratios are divided by the advance ratio at which the coefficient of torque is a minimum. The data on the Bristol 171, Mk. 3, is given in Table 10. The comparison of the power required for the two helicopters is given in Figure 17.

Table 8. Performance Parameters Versus Forward Velocity

V	μ	v_a	C_T	θ_y	α_w	a_o	D_f	L_w	HP_{req_t}	HP_{req}
0	0.0	0.0	0.00184	3.00°	8.93°	0.258°	0.0	0.0	3.50	57.90
20	0.0332	0.00169	0.00172	2.91°	8.84°	0.250°	- 43.0	16.4	3.35	42.37
40	0.0667	0.00268	0.00163	2.31°	8.24°	0.237°	- 32.0	63.0	2.83	27.33
60	0.0999	0.00223	0.00149	1.28°	7.21°	0.218°	- 17.4	132.5	2.11	23.76
80	0.1333	- 0.00077	0.00132	- 0.33°	5.60°	0.195°	1.0	210.0	1.32	21.86
100	0.1665	- 0.00718	0.00122	- 2.47°	3.46°	0.184°	23.0	263.0	0.38	24.13
120	0.1990	- 0.01720	0.00119	- 4.93°	1.00°	0.187°	48.5	274.0	- 0.2	32.13
140	0.2310	- 0.02880	0.00128	- 7.10°	- 1.17°	0.187°	76.9	231.5	- 0.7	44.73

Table 9. Torque Versus Advance Ratio of Proposed Design

μ	$HP_{required}$	C_{Q_E}	$\mu/\mu_{min.C_Q}$	C_Q/C_{Q_o}
0.0	57.90	0.0021	0.0	1.0
0.0332	42.37	0.00153	0.249	0.729
0.0667	27.3	0.000992	0.500	0.472
0.0999	23.76	0.000862	0.748	0.411
0.1333	21.86	0.000794	1.000	0.378
0.1665	24.13	0.000876	1.250	0.417
0.1990	32.13	0.001166	1.493	0.555
0.2310	44.73	0.001623	1.732	0.825

Table 10. Torque Versus Advance Ratio of Bristol 171, Mk. 3

μ	C_Q	$\mu/\mu_{min.C_Q}$	C_Q/C_{Q_o}
0.0	0.00355	0.0	1.0
0.05	0.00290	0.375	0.817
0.10	0.00210	0.752	0.592
0.15	0.00205	1.128	0.578
0.20	0.00238	1.504	0.670
0.25	0.00300	1.880	0.845

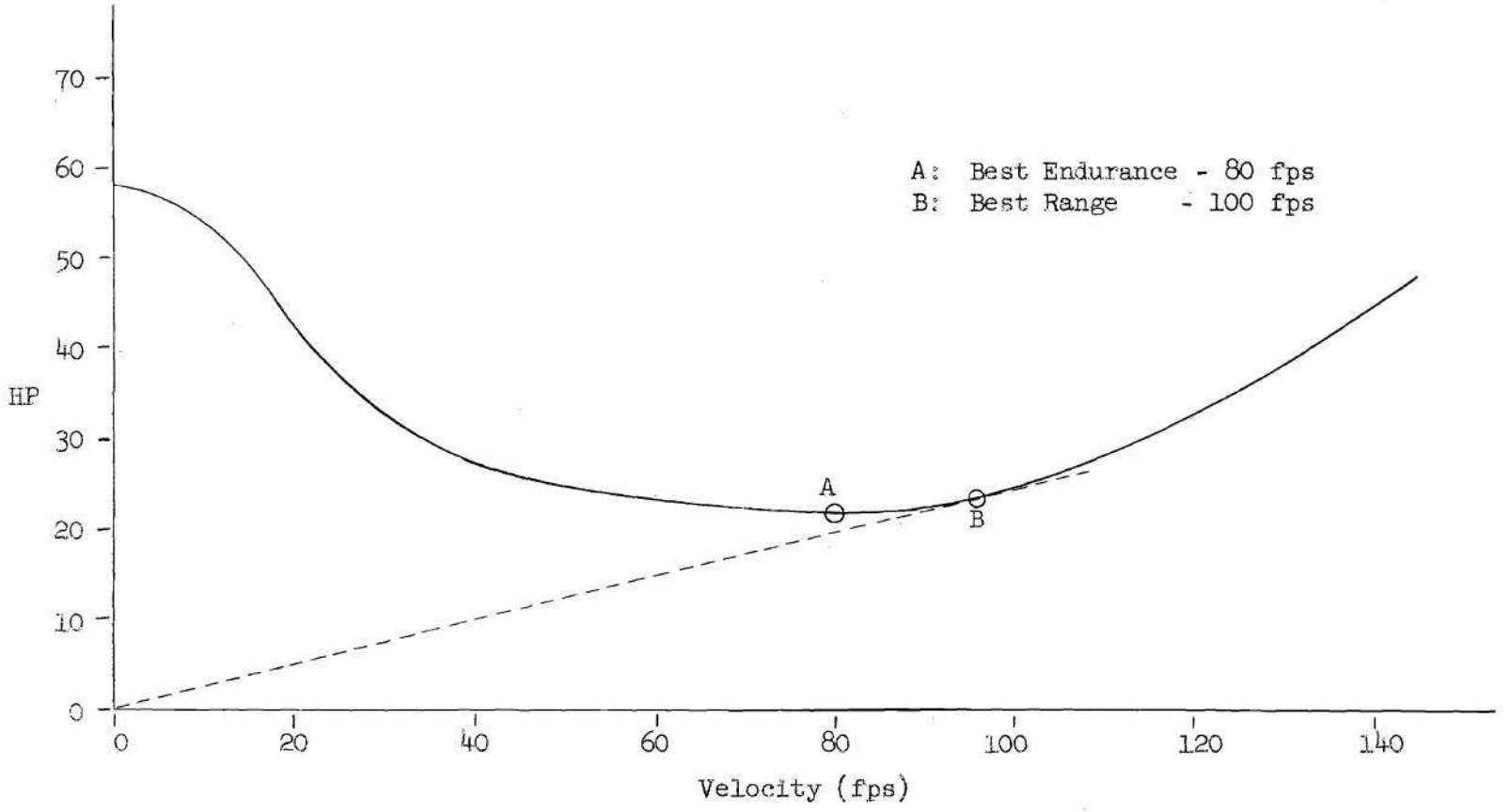

Figure 16. Horsepower Versus Forward Velocity

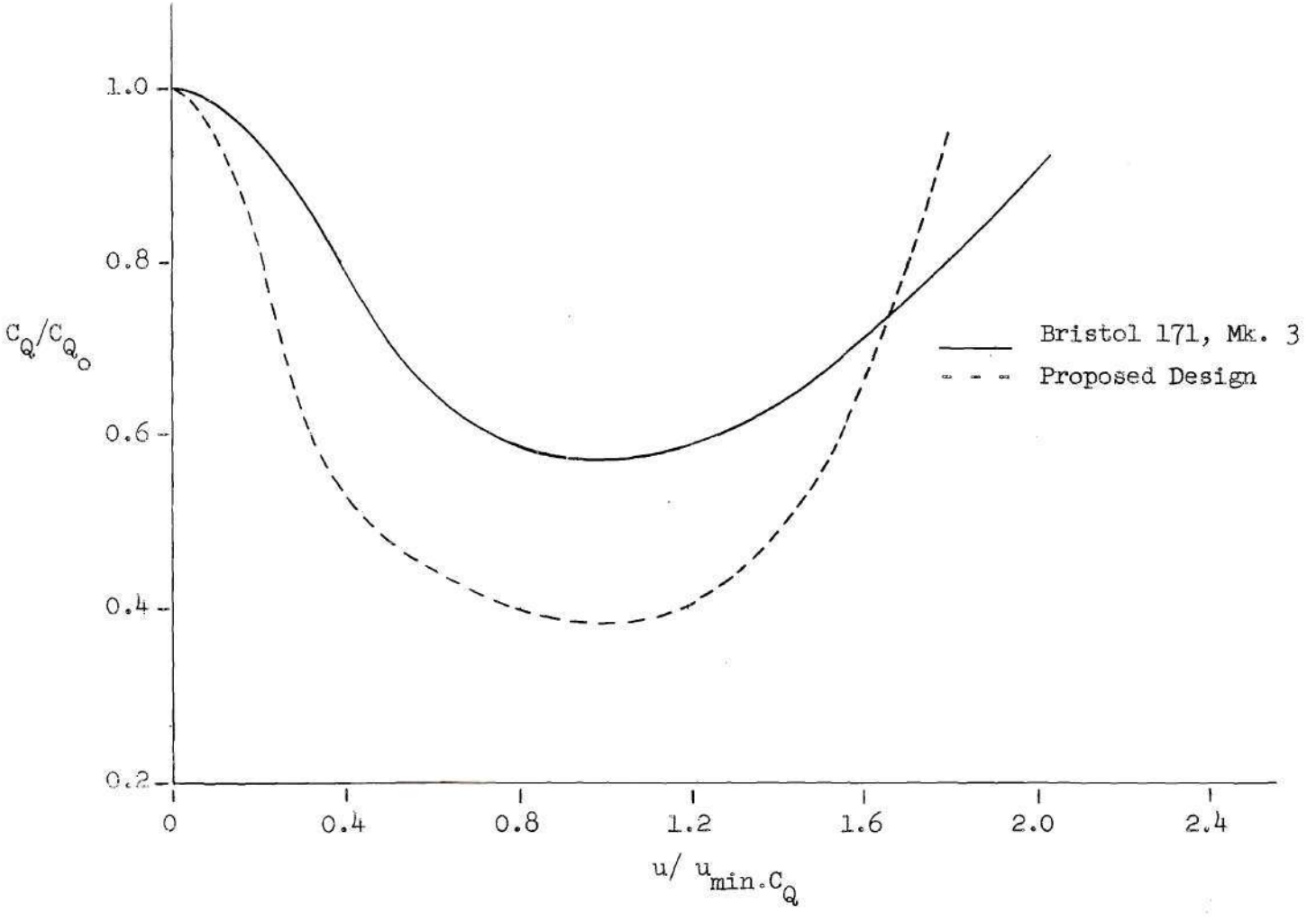

Figure 17. Comparison of Power Required Versus Advance Ratio

APPENDIX X

ESTIMATION OF SHROUDED PROPELLER PARAMETERS

In the discussion of the contribution of the shrouded tail propeller to stability in Chapter VI, it was pointed out that a complete analysis of a shrouded propeller operating in the desired range was not available. Figure 18 shows that the shrouded propeller of the selected reference, NACA 3547, (solid line) falls within the thrust to advance ratios of shrouded propellers having higher static thrust coefficients as given in the report by Theodorsen. It further shows that this will be a conservative estimate of the thrust when compared with a design that it optimized for the desired range of operation (dashed line) (40).

The stability derivatives were determined from non-dimensionalized plots of the shrouded propeller moment and normal force. Since the velocities associated with small disturbances from hovering flight will be in the lower range of the advance ratio, the slopes will be approximated near static conditions. Thus, from Figure 19,

$$\frac{d\,\frac{M}{T_o c}}{d\,\frac{V}{nd}} = 0.906$$

or when converted to the shroud of the proposed design

$$\frac{d\,M_t}{d\,V_t} = 0.530$$

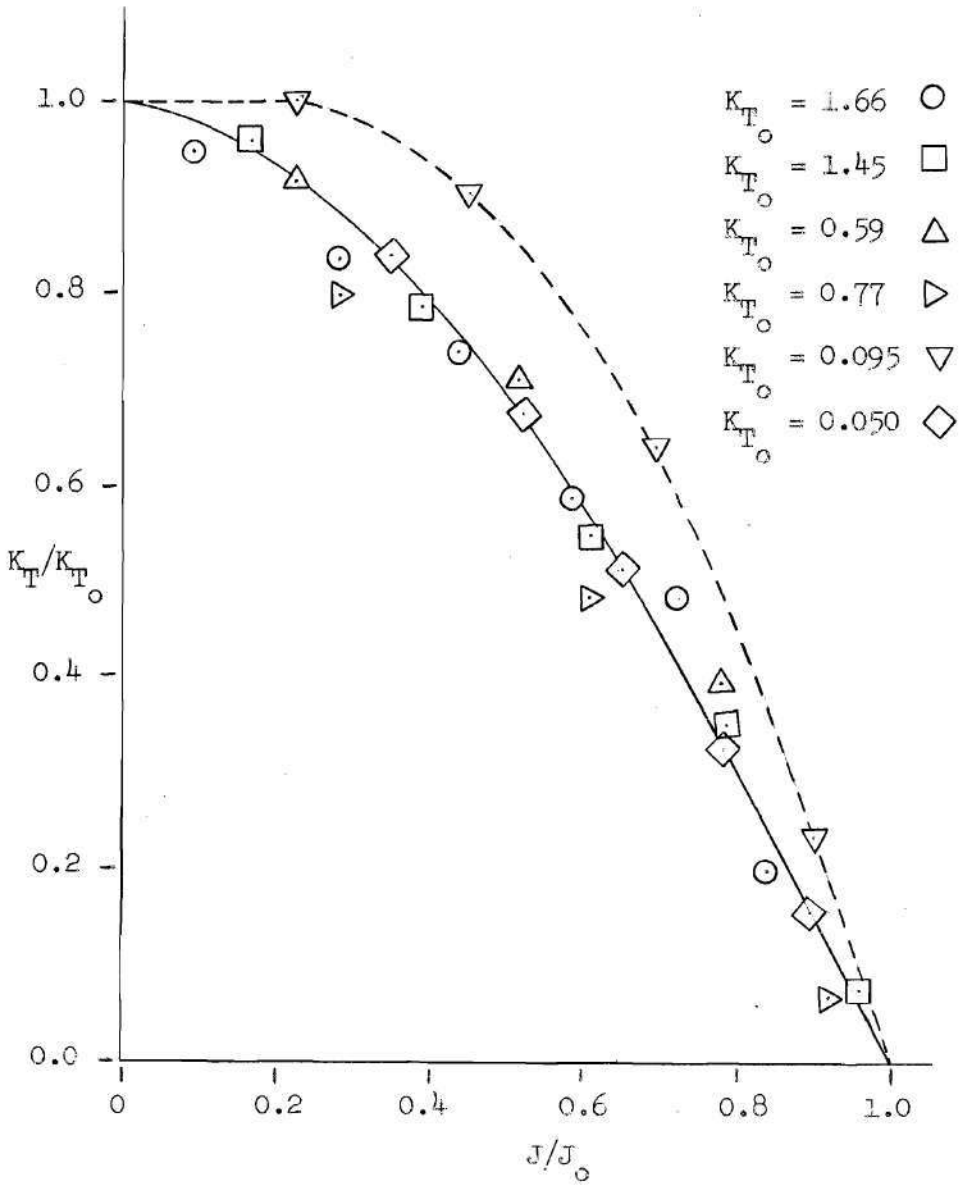

Figure 18. Shroud Thrust Versus Advance Ratio

Since the normal force is a stabilizing force, it was found that the inefficient shroud of NACA TN 3547 gave too great a normal force to be conservative, so data from NASA TN D-995 was used to determine the variation of this force with velocity. The derivative was found to be

$$\frac{d N_t}{d V_t} = 0.70$$

Similarly, from the figure of the non-dimensionalized moment, and normal force versus angle of attack of the tail shroud, the remaining stability derivatives were determined giving

$$\frac{\partial M_t}{\partial \theta} = 7.24$$

and

$$\frac{\partial N_t}{\partial \theta} = 47.3$$

Since these derivatives are also a function of advance ratio, the curves were drawn for an average advance ratio for a small disturbance from hovering flight.

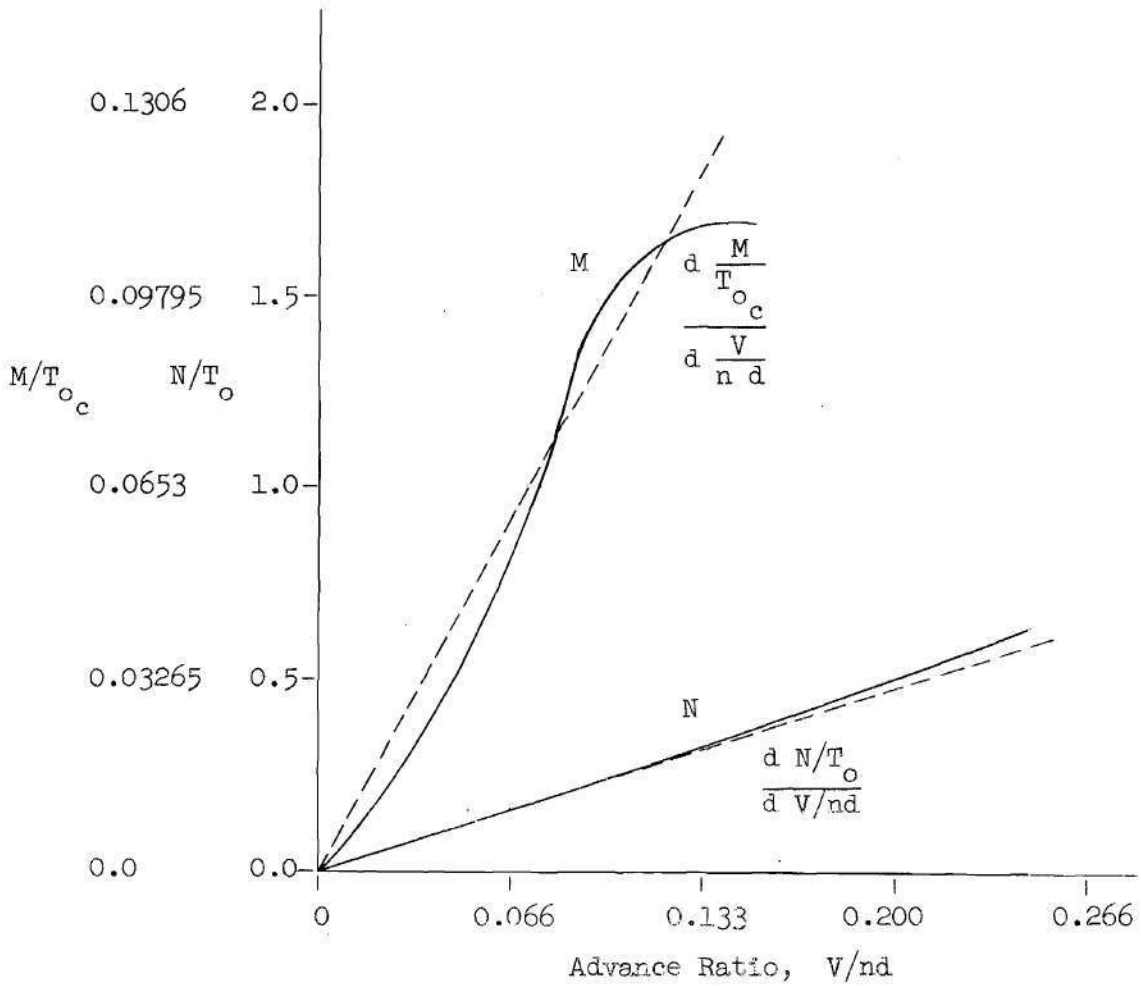

Figure 19. Shroud Parameters Versus Advance Ratio

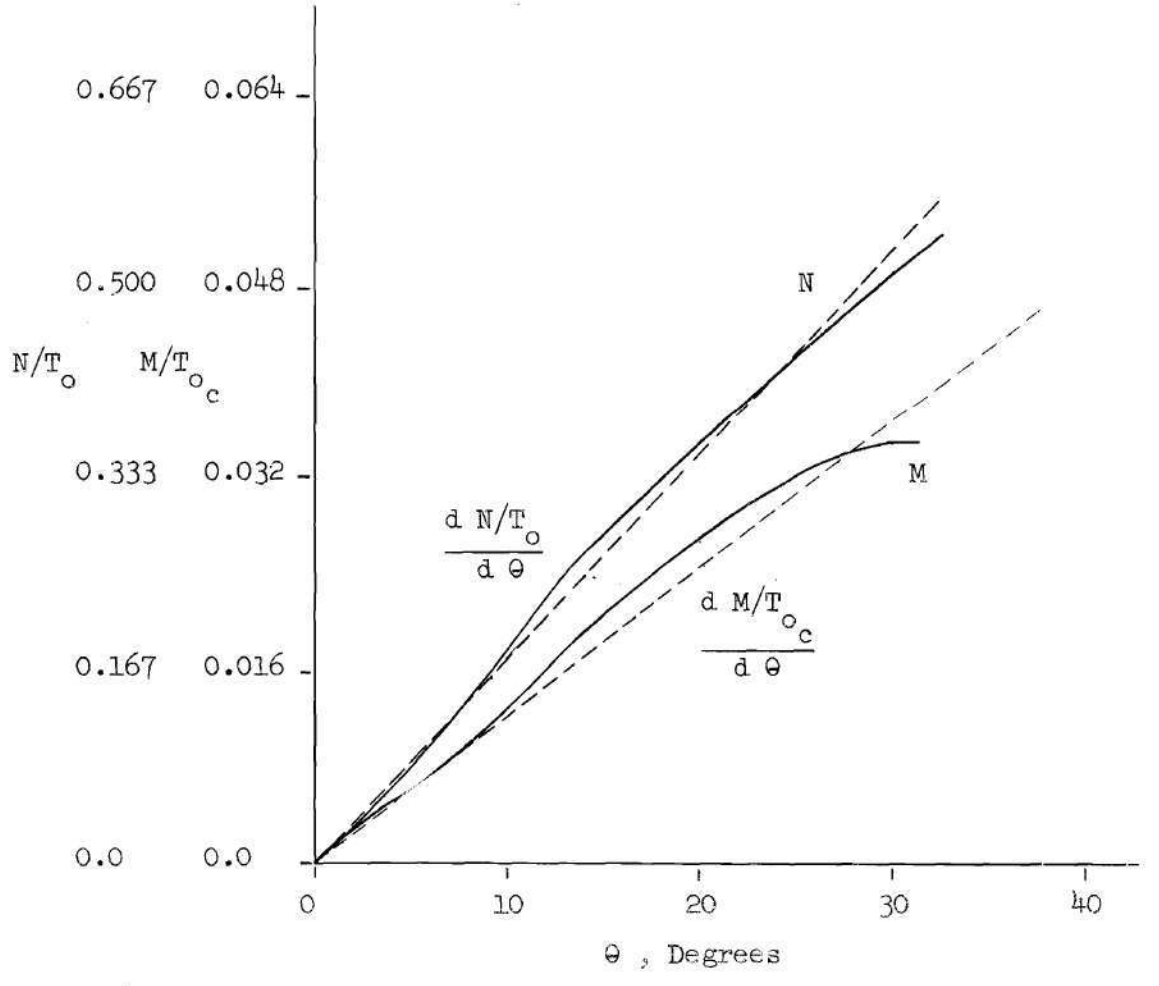

Figure 20. Shroud Parameters Versus Angle of Attack

LITERATURE CITED

1. D. N. Ahnstrom, The Complete Book of Helicopters, The World Publishing Company, New York, 1954, p. 29.

2. Ibid., p. 38.

3. A. A. Nikolsky, Helicopter Analysis, John Wiley and Sons, Inc., New York, 1951, p. 44.

4. A. Gessow and G. C. Myers, Jr., Aerodynamics of the Helicopter, The MacMillan Company, New York, 1957, p. 53.

5. Ibid., p. 64.

6. Ibid., p. 58.

7. Ibid., p. 322.

8. Ibid., p. 194.

9. Ibid., p. 276.

10. Ibid., p. 193.

11. D. O. Dommasch, Elements of Propeller and Helicopter Aerodynamics, Pitman Publishing Corporation, New York, 1953, p. 76.

12. Ibid., p. 77.

13. P. R. Payne, Helicopter Performance and Aerodynamics, Sir Isaac Pitman and Sons, Ltd., London, 1959, p. 103.

14. Ibid., p. 5.

15. E. Jacobs, K. Ward, and R. Pinkerton, The Characteristics of 78 Related Airfoil Sections from Tests in the Variable-Density Wind Tunnel, National Advisory Committee for Aeronautics, Technical Report No. 460, 1933, p. 36.

16. "The McCulloch Engine," Sport Aviation, Vol. II, No. 8, August, 1962, p. 41.

17. S. C. Stevens, A Method for Estimating Performance of Single Rotor Helicopters, Unpublished Master's Thesis, Georgia Institute of Technology, Atlanta, Georgia, 1959, pp.81-104.

18. Gessow, op. cit., p. 113.

19. C. D. Perkins and R. E. Hage, Airplane Performance Stability and Control, John Wiley and Sons, Inc., New York, 1960, p. 73.

20. Stevens, op. cit., p. 27.

21. Payne, op. cit., p. 263.

22. Ibid., p. 263.

23. Ibid., p. 255.

24. Ibid., p. 113.

25. Ibid., p. 124.

26. Ibid., p. 273.

27. Ibid., p. 270.

28. T. Theodorsen, Theoretical Investigation of Ducted Propeller Aerodynamics, Republic Aviation Corporation, Long Island, New York, Vol. II, 1960, p. 284.

29. Payne, op. cit., p. 255.

30. Perkins, op. cit., p. 40.

31. Gessow, op. cit., p. 289.

32. Payne, op. cit., p. 269.

33. Ibid., p. 259.

34. Gessow, op. cit., p. 308.

35. Payne, op. cit., p. 277.

36. Gessow, op. cit., p. 158.

37. S. F. Hoerner, Fluid-Dynamic Drag, Published by the Author, 1958, p. 1-8.

38. Gessow, op. cit., p. 238.

39. Payne, op. cit., p. 214.

40. Theodorsen, op. cit., p. 284.

BIBLIOGRAPHY

1. Abbott, I. H., and Von Doenhoff, A. E., Theory of Wing Sections, Dover Publications, Inc., New York, 1959.

2. Ahnstrom, D. N., The Complete Book of Helicopters, The World Publishing Company, New York, 1954.

3. Castles, W., Jr., Helicopter Performance Estimates, Unpublished Class Notes, Georgia Institute of Technology, 1959.

4. Castles, W., Jr., and Gray, R. B., An Investigation of an Approach to the Problem of Determining the Optimum Design of Shrouded Propellers, Engineering Experiment Station, Georgia Institute of Technology, Atlanta, Georgia, May, 1960.

5. Dommasch, D. O., Elements of Propeller and Helicopter Aerodynamics, Pitman Publishing Corporation, New York, 1953.

6. Gessow, A., and Myers, G. C., Jr., Aerodynamics of the Helicopter, The MacMillan Company, New York, 1957.

7. Grunwald, W. J., and Goodson, K. W., Aerodynamic Loads on an Isolated Shrouded-Propeller Configuration for Angles of Attack from -10° to 110°, National Aeronautics and Space Administration, Technical Note No. D-995, Washington, 1962.

8. Gustafson, F. B., and Reeder, J. P., Helicopter Stability, National Advisory Committee for Aeronautics, Research Memorandum No. L7K04, Washington, 1948.

9. Hoehne, V. O., Shrouded Propeller Investigations: Wind Tunnel Tests of a 2-Bladed Shrouded Propeller Model, University of Wichita Engineering Report No. 213-11, Wichita, Kansas, 1960.

10. Hoerner, S. F., Fluid-Dynamic Drag, Published by the Author, 1958.

11. Jacobs, E., Ward, K., and Pinkerton, R., The Characteristics of 78 Related Airfoil Sections from Tests in the Variable-Density Wind Tunnel, National Advisory Committee for Aeronautics, Technical Report No. 460, 1933.

12. Kruger, W., On Wind Tunnel Tests and Computations Concerning the Problem of Shrouded Propellers, Translation of ZWB Forschungsbericht Nr. 1949, National Advisory Committee for Aeronautics, Technical Memorandum No. 1202, Washington, 1949.

13. Nikolsky, A. A., Helicopter Analysis, John Wiley and Sons, Inc., New York, 1951.

14. Parlett, L. P., Aerodynamic Characteristics of a Small-Scale Shrouded Propeller at Angles of Attack from 0° to 90°, National Advisory Committee for Aeronautics, Technical Note No. 3547, Washington, 1955.

15. Payne, P. R., Helicopter Dynamics and Aerodynamics, Sir Isaac Pitman and Sons, Ltd., 1959.

16. Perkins, C. D., and Hage, R. E., Airplane Performance Stability and Control, John Wiley and Sons, Inc., New York, 1960.

17. Reeder, J. P., and Gustafson, F. B., On the Flying Qualities of Helicopters, National Advisory Committee for Aeronautics, Technical Note No. 1799, Washington, 1949.

18. Stevens, S. C., A Method for Estimating Performance of Single Rotor Helicopters, Unpublished Master's Thesis, Georgia Institute of Technology, 1959.

19. "The McCulloch Engine," Sport Aviation, Volume 11, No. 8, August, 1962.

20. Theodorsen, T., Theoretical Investigation of Ducted Propeller Aerodynamics, Republic Aviation Corporation, Long Island, New York, Vol. II, 1960.

21. Von Mises, R., Theory of Flight, Dover Publications, Inc., New York, 1959.

22. Wood, K. D., Airplane Design, Published by the Author, Boulder, Colorado, 1949.

23. Younger, J. E., Aircraft Tubing Data, Summerill Tubing Company, June, 1943.